Time-dependent Variational Principles for Hybrid Non-Unitary Dynamics: Application to Driven-Dissipative Superconductors

Pasquale Filice,[1] Marco Schirò,[2] and Giacomo Mazza[1]

[1] Dipartimento di Fisica dell'Università di Pisa, Largo Bruno Pontecorvo 3, I-56127 Pisa, Italy
[2] JEIP, UAR 3573 CNRS, Collège de France, PSL Research University, 75321 Paris Cedex 05, France

We introduce time-dependent variational principles to study the non-unitary dynamics of open quantum many-body systems, including dynamics described by the full Lindblad master equation, the non-Hermitian dynamics corresponding to the no-click limit of the fully post-selected quantum trajectories, and the dynamics described by a hybrid Lindbladian with a control parameter α which interpolates between the full post-selection and averaging over all quantum trajectories. As an application we study the non-unitary dynamics of a lossy or driven-dissipative BCS superconductors, evolving in presence of two-body losses and two-body pumps. We show that the non-Hermitian limit acts as a singular limit of the hybrid dissipative dynamics, leading to a sharp modification of the universal approach to the driven-dissipative steady-states. By considering the dissipative dynamics with pair losses, we show that, as the non-Hermitian limit is approached, the density dynamics sharply evolves from a universal power-law to exponential decay that converges towards a quasi-steady plateau characterized by the freezing of the particle depletion due to pair losses. The reached quasi-stationary density increases as a function of the dissipation rate highlighting the emergence of a non-Hermitian Zeno effect in the lossy dynamics. For the driven-dissipative case, we show that, in the non-Hermitian limit, the system gets trapped into an effective negative temperature state, thus skipping the infinite temperature steady-state reached in the presence of finite contribution of the quantum jumps. We rationalize these findings in terms of the conservation of the length of the pseudospins which, in the non-Hermitian limit, suppresses the effective single-particle losses and pumps acting on the non-condensed particles.

I. INTRODUCTION

The dynamics of open quantum systems have attracted the interest of a broad community for several decades now, starting with basic questions on decoherence in quantum mechanics [1–3]. In more recent years the experimental developments of controlled quantum simulators based on ultracold atoms in optical lattices and tweezers, superconducting circuits and trapped ions, have focused the interest on dissipation on quantum many-body systems [4]. Solving the dynamics of a quantum many-body system coupled to an environment represents a major computational and conceptual challenge, one for which the development of quantum computers could naturally provide an advantage [5, 6].

The dynamics of an open quantum systems is encoded in the non-unitary temporal evolution of the reduced density matrix which is obtained by tracing the quantum state of the globally isolated system over the environment. Markovian systems represent an important class of open quantum systems in which the non-unitary dynamics of the reduced density matrix is described by the Lindblad master equation formalism [7]. From a microscopic point of view, the Lindblad master equation can be explicitly derived upon tracing out a specific environment in the so-called Born-Markov approximation [3, 8]. Alternatively, the Lindblad dynamics naturally emerges in the context of the monitored dynamics where it can be obtained as an unraveling over stochastic quantum trajectories describing the conditional evolution of the system under a series of measurement outcomes (quantum jumps) [9–11]. The full post-selection of quantum trajectories with no jumps, also known as the no-click limit [12], represents a specific limit of the monitored dynamics in which the dynamics evolves accordingly to a purely deterministic NHH. Non-Hermitian (NH) quantum many-body systems have been the focus of several theoretical and methodological works [13–26].

A natural interpolation between the full Lindblad evolution and the no-click limit is obtained by introducing hybrid Liouvillians characterized by a control parameter that weights the quantum jumps contribution on the deterministic (unconditional) dynamics. Hybrid Lindbladians admit natural physical interpretations in term of the monitored dynamics such as, for example, a partial post-selection of the measurement outcomes [11, 27], or in terms of the full-counting statistics associated with the number of clicks [28, 29]. In this context, important questions concern the role of quantum jumps for both the conditional and the unconditional dynamics, such as, for example, the extent to which the fully post-selected deterministic NH evolution can be representative of the full Lindblad dynamics or the quantum trajectories [30].

In recent years, several methods have been developed to tackle open quantum many-body systems in various setups [31]. Examples include diagrammatic and renormalization group approaches [32], tensor networks [33–39], semiclassical methods [40, 41], Faber polynomials [25], as well as neural network states [42–45].

In the context of the non-equilibrium dynamics of quantum many-body systems, time-dependent variational methods are particularly appealing for their physical transparency and flexibility. For example, in the unitary case, they have been successfully used to describe the dynamics of both weakly and strongly correlated electrons [46–49]. So far, variational approaches to dissipative systems focused almost exclusively on the steady-state properties [50], whereas time-dependent variational Lindbald dynamics have been recently discussed within phase space methods [51] or in the context of dissipative superconductors [52] and impurity models [53].

In this work we introduce a general class of time-dependent variational principles to describe dynamics in various types of open quantum systems problems, including the Lindblad evolution, its fully post-selected version described by a NHH or the dynamics under partial post-selection, described by hybrid Liouvillians. The variational principles represents the extension to the non-unitary case of the action-based Dirac-Frenkel variational principle for unitary dynamics and allows to derive effective Liouvillians taking into account the many-body nature of the dissipators. We apply our formalism to driven-dissipative BCS superconductors [52, 54–57], relevant, for example, for the dynamics of ultracold superfluid fermions in presence of particle losses [58] or for quantum analogue simulators in cavity QED setups [59]. We discuss the crossover of the non-unitary dynamics from the Lindbald to the fully post-selected NH limit in the case of two-body losses and the driven-dissipative case of simultaneous two-body pumps and losses. We show that, due to the suppression of effective single particle dissipation, the no-click limit represents a singular limit of the non-unitary dynamics in which both the universal approach to the steady state and the steady state itself are sharply modified.

The manuscript is organized as follows. In Sec. II, we introduce the basic formalism of open quantum systems that will be used throughout this work. In Sec. III, we introduce the time-dependent variational principles for the hybrid non-unitary dynamics of dissipative fermions. In Sec. IV, we show the detailed application of the time-dependent variational principles to the driven-dissipative BCS superconductors, and in Sec. V, we present our results for the hybrid non-unitary dynamics in the presence of both two-body losses and pumps. Finally, in Sec. VI we summarize the results of this work and draw our conclusions.

II. HYBRID NON-UNITARY DYNAMICS OF OPEN QUANTUM SYSTEMS

In this section we recall the basics of the dynamics of open quantum systems, from Lindblad evolution to the non-Hermitian dynamics [4]. We focus on the dynamics of open quantum many-body systems described by a Hamiltonian $\mathcal{H}$ and a set of independent environments. In practice, we will always assume a Markovian description of the environments. In this limit, the non-unitary dynamics of the system, obtained upon tracing out the environments, is naturally modeled by the Lindblad master equation

$$d\rho(t) = -idt\,[\mathcal{H},\rho] + dt\sum_\mu \left(L_\mu\rho(t)L_\mu^\dagger - \frac{1}{2}\left\{L_\mu^\dagger L_\mu,\rho\right\}\right), \tag{1}$$

where $\rho(t)$ represents the density matrix of the system. The first term on the right-hand side of Eq. (1) describes the coherent dynamics driven by the Hamiltonian. The second term represents the dissipative (non-unitary) component of the Lindblad equation defined by a set of jump operators L_μ accounting for the effect of the environments on the system.

The two terms entering the dissipative component of the Lindblad equation can be interpreted more clearly by unravelling the dynamics of the reduced density matrix into quantum trajectories. Quantum trajectories are pure states $|\psi(\xi_t,t)\rangle$ that evolve accordingly to the following stochastic Schrödinger equation (SSE) defined by a set of statistically independent Poisson processes $\xi_t=\{\xi_{\mu,t}\}$,

$$\begin{aligned} d|\psi(\xi_t,t)\rangle = &-idt\left[\mathcal{H} - \frac{i}{2}\sum_\mu\left(L_\mu^\dagger L_\mu - \langle L_\mu^\dagger L_\mu\rangle_t\right)\right]|\psi(\xi_t,t)\rangle \\ &+\sum_\mu\left(\frac{L_\mu}{\sqrt{\langle L_\mu^\dagger L_\mu\rangle_t}} - 1\right)d\xi_{\mu,t}|\psi(\xi_t,t)\rangle, \end{aligned} \tag{2}$$

where $\langle\circ\rangle_t \equiv \langle\psi(\xi_t,t)|\circ|\psi(\xi_t,t)\rangle$, $d\xi_{\mu,t}d\xi_{\mu',t} = \delta_{\mu\mu'}d\xi_{\mu,t}$ and $d\xi_{\mu,t}\in\{0,1\}$ with expectation values $E\left[d\xi_{\mu,t}\right] = dt\langle L_\mu^\dagger L_\mu\rangle_t$. The dynamics of a single quantum trajectory breaks down into two steps: a deterministic non-unitary evolution governed by the NHH

$$\mathcal{H}_{\mathrm{nH}} = \mathcal{H} - \frac{i}{2}\sum_\mu L_\mu^\dagger L_\mu, \tag{3}$$

corresponding to the so-called recycling term in Eq. 1 written in terms of anticommutator, and a series of stochastic quantum jumps at random times (second line of Eq. (2)), at which the state $|\psi(\xi_t,t)\rangle$ changes discontinuously. We note that the stochastic evolution is normalised and state dependent, as is evident from the expectation values $\langle L_\mu^\dagger L_\mu\rangle_t$ appearing in both the deterministic and the stochastic parts of Eq. (2), and in the rates of the Poisson processes. Given a quantum trajectory, one can define the conditional density matrix $\rho_c(\xi_t,t) = |\psi(\xi_t,t)\rangle\langle\psi(\xi_t,t)|$. Considering all possible quantum trajectories, the density matrix averaged over all measurement outcomes

$$E\left[\rho(t)\right] \equiv \lim_{N_\xi\to\infty}\frac{1}{N_\xi}\sum_{\xi_t}\rho_c(\xi_t,t), \tag{4}$$

evolves according to the Lindblad master equation in Eq. (1). On the contrary, if one post-selects the quantum trajectories over the records of no clicks, the dynamics is deterministic and completely governed by $\mathcal{H}_{\mathrm{nH}}$.

An intermediate case between the Lindblad evolution and no-click limit is obtained by defining the temporal evolution of the density matrix accordingly to a modified Lindbladian parametrized by a real parameter $\alpha \in [0,1]$

$$d\rho_\alpha(t) = dt\mathcal{L}_\alpha[\rho_\alpha(t)] \tag{5}$$

with

$$\mathcal{L}_\alpha = -i\left[\mathcal{H}, \rho_\alpha(t)\right] + \delta\mathcal{L}_\alpha[\rho_\alpha(t)] \tag{6}$$

and dissipator

$$\delta\mathcal{L}_\alpha = \sum_\mu \left(\alpha L_\mu \rho_\alpha(t) L_\mu^\dagger - \frac{1}{2}\left\{L_\mu^\dagger L_\mu, \rho_\alpha\right\}\right). \tag{7}$$

The hybrid dissipator in Eq. (7) interpolates between the full Lindblad dynamics for $\alpha = 1$ and the post -selected no-clicks non-Hermitian evolution for $\alpha = 0$. For later convenience, we notice that the hybrid dissipator can be equivalently written in the form of a full Lindblad dissipator with renormalized coupling supplemented by a purely non-Hermitian contribution

$$\delta\mathcal{L}_\alpha = \alpha\delta\mathcal{L}_1 + \frac{1}{2}(\alpha - 1)\sum_\mu \left\{L_\mu^\dagger L_\mu, \rho_\alpha\right\}, \tag{8}$$

where $\delta\mathcal{L}_1 \equiv \delta\mathcal{L}_{\alpha=1}$.
Equations (5)-(7) define the general form of hybrid Liouvillians considered in this work. We notice that, for any value $0 \le \alpha < 1$, namely for all cases except for the Lindblad one $\alpha = 1$, the dynamics governed by the hybrid Liouvillian does not conserve the norm. We therefore include an explicit normalization in the definition of the expectation values, *i.e.*

$$\langle\hat{O}\rangle_\alpha(t) \equiv \frac{\mathrm{Tr}\left(\rho_\alpha(t)\hat{O}\right)}{\mathrm{Tr}\left(\rho_\alpha(t)\right)} \tag{9}$$

This in fact comes naturally from the interpretation of quantum trajectories as measurement problem: after any non-unitary step, either a click or a no-click, the state is properly normalized as enforced both for the quantum jump term as well as for the non-Hermitian evolution in Eq. (2). Assuming the hybrid Liouvillian evolution Eq. (5), the equations of motion for the expectation values $\langle\hat{O}\rangle_\alpha$ read

$$\begin{aligned}\frac{d\langle\hat{O}\rangle_\alpha}{dt} &= -i\langle\left[\hat{O}, \mathcal{H}\right]\rangle_\alpha \\ &+ \frac{\alpha}{2}\sum_\mu\left(\langle L_\mu^\dagger\left[\hat{O}, L_\mu\right]\rangle_\alpha - \langle\left[\hat{O}, L_\mu^\dagger\right]L_\mu\rangle_\alpha\right) \\ &+ \frac{\alpha-1}{2}\sum_\mu\left(\langle\left\{L_\mu^\dagger L_\mu \hat{O}\right\}\rangle_\alpha - 2\langle L_\mu^\dagger L_\mu\rangle_\alpha\langle\hat{O}\rangle_\alpha\right),\end{aligned} \tag{10}$$

where the last term comes from the normalization introduced in Eq. (9). We observe that the same equations of motions can be equivalently obtained by supplementing the hybrid Liouvillian with non-linear term

$$\bar{\mathcal{L}}_\alpha = \mathcal{L}_\alpha - \rho_\alpha(\alpha - 1)\sum_\mu\langle L_\mu^\dagger L_\mu\rangle_\alpha, \tag{11}$$

such that $\mathrm{Tr}\left[\bar{\mathcal{L}}_\alpha\right] = 0$ the resulting dynamics is norm conserving. By taking the $\alpha = 0$ limit, it is immediate to check that the non-linear term in Eq. (11) is equivalent to the normalization introduced for the stochastic Schrödinger equation in the no-click limit.

III. TIME-DEPENDENT VARIATIONAL PRINCIPLES

In this section, we introduce a class of time-dependent variational principles for the hybrid non-unitary dynamics. We consider variational principles defined by the application of stationary conditions on suitably defined actions. In the case of unitary dynamics, the variational dynamics is expressed by the Dirac-Frenkel variational principle (DFVP), defined by the action

$$\mathcal{S}_{\mathrm{DF}} = \int dt\langle\Psi(t)|i\partial_t - H|\Psi(t)\rangle \tag{12}$$

and the stationary condition $\delta\mathcal{S}_{\mathrm{DF}} = 0$. Eq. (12) can be viewed as the least action definition of the time-dependent Schrödinger equation. Here, we extend this concept to the non-unitary case. We start from the full Lindbald dynamics $\alpha = 1$ and introduce an action $\mathcal{S}[\rho_v, \rho_{\mathrm{aux}}]$ which is a functional of a variational state $\rho_v(t)$ and of an auxiliary state $\rho_{\mathrm{aux}}(t)$

$$\mathcal{S}[\rho_v, \rho_{\mathrm{aux}}] = \int dt\mathrm{Tr}\left[\rho_{\mathrm{aux}}\left(\partial_t\rho_v(t) - \mathcal{L}_1[\rho_v(t)]\right)\right]. \tag{13}$$

Starting from the action Eq. (13), we define the density matrix variational principle (DMVP) by requiring the stationarity of the action with respect to the auxiliary state, *i.e.*

$$\frac{\delta\mathcal{S}[\rho_v, \rho_{\mathrm{aux}}]}{\delta\rho_{\mathrm{aux}}} = 0. \tag{14}$$

Analogously to the DFVP, the DMVP in Eq. (14) can be viewed as a least action definition of the Lindblad master equation. The choice of the auxiliary state is completely arbitrary and it is formally introduced to take the variation of the action. In particular, the choice of ρ_{aux} does not affect the variational freedom of the problem. On the contrary, the variational freedom is constrained by the the choice of the specific variational density matrix $\rho_v(t)$ that, for an arbitrary ρ_{aux}, defines the action associated with the variational state. We notice that, upon introducing the vectorization (or superfermion) formalism, where the Lindblad superoperator becomes a non-Hermitian matrix acting on vectorized density matrices [60, 61], the DMVP can be recast in a similar form to the DFVP

$$\mathcal{S} = \int dt \, \langle\langle \rho_{aux} \, | \, \partial_t - \tilde{\mathcal{L}} \, | \rho_v \rangle\rangle \tag{15}$$

where the symbol $|\rangle\rangle$ indicates vectors in the product Hilbert space and $\tilde{\mathcal{L}}$ is the superoperator definition of the Liouvillian. The DMVP is therefore obtained by taking the variation with respect to the bra-vector $\delta\mathcal{S}/\delta \langle\langle \rho_{aux} \, | = 0$.
The DMVP can be readily extended to the hybrid case $\alpha \neq 1$. In this case, the variational principle must include also the state normalization. Following the discussion of the previous section, the are two equivalent ways of extending the DMVP to the case of the hybrid Liouvillian by keeping into account the state normalization. In the first case, one uses the original, *i.e.* non norm-conserving, hybrid Liouvillian Eq. (6) and explicitly normalizes all the traces with respect to the trace of the variational density matrix. Specifically, the DMVP becomes

$$\frac{\delta}{\delta \rho_{\rm aux}} \int \frac{\mathrm{Tr}\left[\rho_{\rm aux}(\partial_t \rho_v(t) - \mathcal{L}_\alpha[\rho_v(t)])\right]}{\mathrm{Tr}\left[\rho_v(t)\right]} = 0. \tag{16}$$

Equivalently, one may consider the non-linear norm conserving hybrid Liouvillian, Eq. (11), and write

$$\frac{\delta}{\delta \rho_{\rm aux}} \int dt \mathrm{Tr}\left[\rho_{\rm aux}\left(\partial_t \rho_v(t) - \overline{\mathcal{L}}_\alpha[\rho_v(t)]\right)\right] = 0. \tag{17}$$

Obviously, Eqs. (16)-(17) reduce to Eq. (14) for $\alpha = 1$.

A. Non-Hermitian Dirac-Frenkel Variational Principle

We now consider the no-click limit, $\alpha = 0$, of the variational non-unitary dynamics. In this limit, the variational dynamics can be equivalently expressed in terms of a non-Hermitian extension of the DFVP (NH-DFVP). The NH-DFVP reads

$$\delta \int dt \langle \Psi(t) | i\partial_t - \mathcal{H}_{\rm nH} | \Psi(t) \rangle + \mu(t) \left(\langle \Psi(t) || \Psi(t) \rangle - 1 \right) = 0, \tag{18}$$

where $\mu(t)$ is a time-dependent Lagrange multiplier ensuring the normalization of the state. Taking the variation with respect to both the state and the Lagrange parameter one obtains $\mu(t) = \frac{i}{2} \sum_\mu \langle \Psi(t) | L_\mu^\dagger L_\mu | \Psi(t) \rangle$ matching the definition of the norm-conserving NHH evolution in the no-click limit of the SSE, see Eqs. (2). It is immediate to check that, by constructing a time-dependent mixed state

$$\rho(t) = \sum_n p_n |\Psi_n(t)\rangle\langle\Psi_n(t)| \tag{19}$$

with $p_n > 0$ and $\sum_n p_n = 1$, and upon extending the definition of the action for the NH-DFVP as

$$\begin{aligned} \mathcal{S}_{NH} = \sum_n p_n \int dt \langle \Psi_n(t) | i\partial_t - \mathcal{H}_{\rm nH} | \Psi_n(t) \rangle \\ + \mu(t) \left(\langle \Psi_n(t) || \Psi_n(t) \rangle - 1 \right), \end{aligned} \tag{20}$$

the stationary condition $\delta \mathcal{S}_{NH} = 0$ leads to the same variational dynamics determined by the DMVP for $\alpha = 0$. We notice that the NH extension of the DFVP can applied in combination with the method of quantum-trajectories to obtain a variational description of the non-unitary dynamics governed by the Stochastic Scrhödinger Equation.

B. Example: Variational Gaussian States

We now show a practical implementation of the above variational principles in the case of Gaussian variational density matrices $\rho_v(t) = \rho_0(t)$. In this case, it is possible to formally calculate the action without an explicit definition of the auxiliary state and by retaining the full functional dependence of the action on $\rho_{\rm aux}$. We consider a Liouvillian built from a generic many-body Hamiltonian of the form

$$\mathcal{H} = \sum_{ab} t_{ab} c_a^\dagger c_b + \frac{1}{2} \sum_{abcd} U_{abcd} c_a^\dagger c_b^\dagger c_c c_d \tag{21}$$

and a many-body jump operator describing two-particle losses

$$L = \sum_{ab} \sqrt{\kappa_{ab}} c_a c_b. \tag{22}$$

Here, $c_a^\dagger$ and c_a are fermionic creation and annihilation operators, and we used latin indexes to label generic quantum numbers associated with the latter. t_{ab} and U_{abcd} are, respectively, the hopping and the interaction matrix elements, and $\sqrt{\kappa_{ab}}$ are the dissipation rates in the ab channel.
We start from the limit $\alpha = 1$ and compute the trace $\mathrm{Tr}\left(\rho_{\rm aux} \mathcal{L}_1[\rho_0(t)]\right)$. As shown in the appendix (A), the gaussianity of the state allows to express this trace in terms of an effective Hartree-Fock single-particle Liouvillian

$$\mathrm{Tr}\left(\rho_{\rm aux} \mathcal{L}_1[\rho_0(t)]\right) = \mathrm{Tr}\left(\rho_{\rm aux} \mathcal{L}_{HF}[\rho_0(t)]\right) \tag{23}$$

with

$$\mathcal{L}_{HF}[\rho_0] = -i\left[\mathcal{H}_{HF}[\rho_0], \rho_0\right] + \delta\mathcal{L}_{HF}[\rho_0]. \tag{24}$$

Here, $\mathcal{H}_{HF}[\rho_0(t)]$ is the usual time-dependent Hartree-Fock single-particle Hamiltonian

$$\mathcal{H}_{HF} = \sum_{ab} t_{ab} c_a^\dagger c_b + \sum_{abcd} V_{abcd} \mathrm{Tr}\left(\rho_0(t) c_a^\dagger c_d\right) c_b^\dagger c_c \tag{25}$$

with $V_{abcd} \equiv U_{abcd} - U_{abdc}$, and $\delta\mathcal{L}_{HF}[\rho_0]$ is an effective Hartree-Fock dissipator which reads

$$\delta\mathcal{L}_{HF} = 2\sum_{abcd} \Gamma_{abcd} \mathrm{Tr}\left(\rho_0(t) c_a^\dagger c_d\right) \delta\mathcal{L}^{cb}[\rho_0], \tag{26}$$

where $\delta\mathcal{L}^{cb}[\rho_0]$ is a single-particle loss dissipator

$$\delta\mathcal{L}^{cb}[\rho_0] = c_c \rho_0 c_b^\dagger - \frac{1}{2}\left\{c_b^\dagger c_c, \rho_0\right\}, \tag{27}$$

and $\Gamma_{abcd} \equiv \sqrt{\kappa_{ba}\kappa_{cd}} - \sqrt{\kappa_{ba}\kappa_{dc}}$. We notice that, due to the many-body nature of the original jump operators, the effective Hartree-Fock single-particle dissipator is characterized by effective couplings which depend on the variational state itself.
By taking the variation of the action defined by Eq. (23) with respect to the auxiliary density matrix ρ_{aux}, we obtain the effective Liouvillian for the variational density matrix

$$\partial_t \rho_0(t) = -i\left[\mathcal{H}_{HF}[\rho_0], \rho_0\right] + \delta\mathcal{L}_{HF}[\rho_0]. \tag{28}$$

Let us now consider the $\alpha < 1$ case. Using the normalized variational principle in Eq. (16), the calculation of the traces on the normalized state is carried out exactly as before, and the effective hybrid Liouvillian for the Gaussian state reads

$$\begin{aligned}\partial_t \rho_{0,\alpha}(t) = &-i\left[\mathcal{H}_{HF}[\rho_{0,\alpha}], \rho_{0,\alpha}\right] + \alpha\delta\mathcal{L}_{HF}[\rho_{0,\alpha}] \\ &+ (\alpha-1)\sum_{abcd}\Gamma_{abcd}\mathrm{Tr}\left(\rho_{0,\alpha}(t) c_a^\dagger c_d\right)\left\{c_b^\dagger c_c, \rho_{0,\alpha}\right\}.\end{aligned} \tag{29}$$

On the other hand, by using the norm-conserving variational principle Eq. (17), the effective hybrid Liouvillian becomes

$$\begin{aligned}\partial_t \overline{\rho}_{0,\alpha}(t) = &-i\left[\mathcal{H}_{HF}[\overline{\rho}_{0,\alpha}], \overline{\rho}_{0,\alpha}\right] + \alpha\delta\mathcal{L}_{HF}[\overline{\rho}_{0,\alpha}] \\ &+ (\alpha-1)\sum_{abcd}\Gamma_{abcd}\Big[\mathrm{Tr}\left(\overline{\rho}_{0,\alpha}(t) c_a^\dagger c_d\right)\left\{c_b^\dagger c_c, \overline{\rho}_{0,\alpha}\right\} \\ &-2(\alpha-1)\overline{\rho}_{0,\alpha}(t)\mathrm{Tr}\left(\overline{\rho}_{0,\alpha}(t) c_a^\dagger c_d\right)\mathrm{Tr}\left(\overline{\rho}_{0,\alpha}(t) c_b^\dagger c_c\right)\Big].\end{aligned} \tag{30}$$

On can readily check the equivalence between Eq. (29) and Eq. (30) by computing the equations of motions for the normalized observables

$$\langle \hat{O}\rangle_\alpha = \frac{\mathrm{Tr}\left(\rho_{0,\alpha}\hat{O}\right)}{\mathrm{Tr}\left(\rho_{0,\alpha}\right)} = \mathrm{Tr}\left(\overline{\rho}_{0,\alpha}\hat{O}\right). \tag{31}$$

IV. DRIVEN-DISSIPATIVE DYNAMICS IN BCS SUPERCONDUCTORS

We now discuss the application of the time-dependent variational principle to the driven-dissipative dynamics in BCS superconductors. We consider a system of spinful fermions hopping on a lattice with local pairing interaction as described by the attractive Hubbard model

$$\mathcal{H} = \sum_{ij\sigma} t_{ij} c_{i\sigma}^\dagger c_{j\sigma} - |U|\sum_i n_{i\uparrow} n_{i\downarrow} \tag{32}$$

where $-|U|$ is the attraction and the t_{ij} the hopping amplitude between sites i and j. We consider a periodic lattice with $t_{ij} = t_{(i-j)}$, and assume that the hopping matrix elements give rise to a band of width W characterized by flat-density density of states.
At equilibrium, the competition between electron hopping and local pairing represents the simplest description of the crossover between weak and strong coupling superconductivity which is relevant in the contexts of high-temperature superconductors and BCS to BEC superfluidity [62–66]. In out of equilibrium conditions, the unitary dynamics is characterized by a series of dynamical phase transitions arising in various quench protocols [67–76]. The effect of two-particle losses has been studied in Ref. 55 by approximation of the full Lindbald by its NH limit, and by the determination of the spectrum of the resulting NHH. Ref. 54 focused on the full Lindblad dissipative dynamics by means of a specific decoupling of the interaction which leads to an effective unitary dynamics with complex pairing interaction. Later on, it was showed that the application of the DMVP to the full Linbladian, see Eq. (14), leads to a much richer dynamics that clearly shows how the non-unitary effects discarded in previous works dominates the dissipative dynamics [52].
Here, we consider the hybrid driven-dissipative dynamics by considering both two-particle losses and pumps

$$\delta\mathcal{L}_{\alpha,\alpha'} = \delta\mathcal{L}_\alpha^{\mathrm{loss}} + \delta\mathcal{L}_{\alpha'}^{\mathrm{pump}} \tag{33}$$

with

$$\delta\mathcal{L}_\alpha^X = \sum_i\left(\alpha L_i^X \rho_\alpha(t) L_i^{X\dagger} - \frac{1}{2}\left\{L_i^{X\dagger} L_i^X, \rho_\alpha\right\}\right) \tag{34}$$

for $X \in (\mathrm{loss}, \mathrm{pump})$, and

$$L_i^{\mathrm{loss}} = \sqrt{2\Gamma} c_{i\downarrow} c_{i\uparrow} \tag{35}$$

and

$$L_i^{\mathrm{pump}} = \sqrt{2P} c_{i\uparrow}^\dagger c_{i\downarrow}^\dagger. \tag{36}$$

In the definition of the dissipator, Eq. (33), we explicitly highlight that, in principle, one may consider different parameters α and α' for the hybrid non-unitary dynamics of losses and pumps. In the following we consider only the case $\alpha = \alpha'$.

A. BCS hybrid Liouvillians

We derive the equation of motions for the hybrid dissipative dynamics by using a BCS ansatz for the variational density matrix. The BCS state is a Gaussian state allowing for non zero anomalous contractions, *i.e.* $\mathrm{Tr}\left(\rho_0 c^\dagger_\uparrow c^\dagger_\downarrow\right) \neq 0$. We use the normalized version of the variational principle, Eq. (16), and we constraint the variational state to preserve translation invariance and spin unpolarized density. By including anomalous contractions in the calculation of the action, we obtain the effective Liouvillian for the BCS state, see appendix B for details. The BCS state evolves with an hybrid effective BCS-Liouvillian

$$\partial_t \rho_{0,\alpha} = \mathcal{L}_{BCS,\alpha}[\rho_{0,a}] \tag{37}$$

with

$$\mathcal{L}_{BCS,\alpha} = -i\left[H_{BCS}(\Gamma,P),\rho_{0,\alpha}\right] + \delta\mathcal{L}^{\rm loss}_{BCS,\alpha} + \delta\mathcal{L}^{\rm pump}_{BCS,\alpha}. \tag{38}$$

The BCS Liouvillian is defined by a unitary BCS Hamiltonian, $H_{BCS}(\Gamma,P)$, which depends on the pump and loss rates, and two effective dissipators which take into account losses and pumps. The unitary Hamiltonian $H_{BCS}(\Gamma,P)$ is obtained by adding to the standard BCS Hamiltonian two complex valued pairing potentials as

$$H_{BCS}(\Gamma,P) = H_{BCS,0}(t) + i(\Gamma-P)\Delta(t)\sum_i c_{i\downarrow}c_{i\uparrow} + \text{h.c.}\,. \tag{39}$$

Here,

$$\Delta(t) \equiv \frac{\mathrm{Tr}\left(\rho_{0,\alpha}(t) c^\dagger_{i\uparrow} c^\dagger_{i\downarrow}\right)}{\mathrm{Tr}\left(\rho_{0,\alpha}\right)} \tag{40}$$

is the superconducting order parameter, and $H_{BCS,0}$ is the usual time-dependent BCS Hamiltonian

$$H_{BCS,0} = \sum_{ij\sigma} t_{ij} c^\dagger_{i\sigma} c_{j\sigma} - |U|\Delta(t)\sum_i c_{i\downarrow}c_{i\uparrow} + \text{h.c.}. \tag{41}$$

The effective dissipators in loss and pump channels read

$$\begin{aligned}\delta\mathcal{L}^{\rm loss}_{BCS,\alpha} &= 2\Gamma\frac{n(t)}{2}\delta L^{1-\rm l}_\alpha[\rho_{0,\alpha}] + \\ &+ 2\Gamma(\alpha-1)\sum_i \Delta(t) c_{i\downarrow}c_{i\uparrow}\rho_{0,a} + \Delta(t)^*\rho_{0,\alpha} c^\dagger_{i\uparrow}c^\dagger_{i\downarrow}\end{aligned} \tag{42}$$

and

$$\begin{aligned}\delta\mathcal{L}^{\rm pump}_{BCS,\alpha} &= 2P\left(1-\frac{n(t)}{2}\right)\delta L^{1-\rm p}_\alpha[\rho_{0,\alpha}] + \\ &+ 2P(\alpha-1)\sum_i \Delta(t)\rho_0 c_{i\downarrow}c_{i\uparrow} + \Delta(t)^* c^\dagger_{i\uparrow}c^\dagger_{i\downarrow}\rho_0\end{aligned} \tag{43}$$

In Eqs. (42)-(43) $\delta\mathcal{L}^{1-\rm l}_\alpha$ and $\delta\mathcal{L}^{1-\rm p}_\alpha$ represent, respectively, hybrid single-particle pump dissipators

$$\delta\mathcal{L}^{1-\rm l}_\alpha = \sum_{i\sigma}\left(\alpha c_{i\sigma}\rho_{0,\alpha}c^\dagger_{i\sigma} - \frac{1}{2}\left\{c^\dagger_{i\sigma}c_{i\sigma},\rho_{0,\alpha}\right\}\right) \tag{44}$$

and

$$\delta\mathcal{L}^{1-\rm p}_\alpha = \sum_{i\sigma}\left(\alpha c^\dagger_{i\sigma}\rho_{0,\alpha}c_{i\sigma} - \frac{1}{2}\left\{c_{i\sigma}c^\dagger_{i\sigma},\rho_{0,\alpha}\right\}\right), \tag{45}$$

and $n(t) = \sum_\sigma \frac{\mathrm{Tr}\left(\rho_{0,\alpha}c^\dagger_{i\sigma}c_{i\sigma}\right)}{\mathrm{Tr}\left(\rho_{0,\alpha}\right)}$ is the total particle density. The loss and pump contributions to the effective Liouvillian are related by the particle-hole transformation $c_{i\sigma} \to c^\dagger_{i\sigma}$. In particular, under particle-hole, the order parameter and the particle density transform, respectively, as $\Delta \to -\Delta^*$ and $n \to 2-n$. It is important to observe that, in Eqs. (42)-(43), the single-particle dissipators are characterized by effective dissipation rates which are proportional to the number of particles (losses) and on the number of holes (pumps). This fact is due to the many-body nature of the jump operators and indicates that the two-body losses (or the two-body pumps) get more and more disfavored as the system get completely depleted (or completely filled).
In the limit $\alpha = 0$, the effective Liouvillian reduces to a non-hermitian BCS (NH-BCS) Hamiltonian

$$\mathcal{L}_{BCS,\alpha}\big|_{\alpha=0} = -iH_{\text{nH}-BCS}\rho_0 + i\rho_0 H^\dagger_{\text{nH}-BCS} \tag{46}$$

with

$$\begin{aligned}H_{\text{nH}-BCS} &= H_{BCS}(\Gamma,P) - i\frac{n}{2}\Gamma\sum_{i\sigma}c^\dagger_{i\sigma}c_{i\sigma} \\ &- i\left(1-\frac{n}{2}\right)P\sum_{i\sigma}c_{i\sigma}c^\dagger_{i\sigma}.\end{aligned} \tag{47}$$

It is immediate to check that the NH-BCS Hamiltonian, Eq. (47), can be also directly obtained from the NH-DFVP Eq. (18) without the use of the auxiliary state $\rho_{\rm aux}$.

B. Equation of motions for normalized observables

We derive the equations of motion for the normalized momentum-dependent density and paring amplitudes

$$n_{\mathbf{k}\sigma} \equiv \frac{\mathrm{Tr}\left(\rho_{0,\alpha}c^\dagger_{\mathbf{k}\sigma}c_{\mathbf{k}\sigma}\right)}{\mathrm{Tr}\left(\rho_{0,\alpha}\right)} \tag{48}$$

and

$$\Delta_{\mathbf{k}} \equiv \frac{\mathrm{Tr}\left(\rho_{0,\alpha}c^\dagger_{\mathbf{k}\uparrow}c^\dagger_{-\mathbf{k}\downarrow}\right)}{\mathrm{Tr}\left(\rho_{0,\alpha}\right)}. \tag{49}$$

From the momentum-dependent observables, the local density and order parameter read

$$n = \sum_{\mathbf{k}\sigma} n_{\mathbf{k}\sigma} \quad \text{and} \quad \Delta = \sum_{\mathbf{k}}\Delta_{\mathbf{k}}. \tag{50}$$

Notice that, by symmetry, $n_{\mathbf{k}\uparrow} = n_{-\mathbf{k}\uparrow} = n_{\mathbf{k}\downarrow}$ and $\Delta_{\mathbf{k}} = \Delta_{-\mathbf{k}}$. The equations of motion reads

$$\partial_t n_{\mathbf{k}\sigma} = \frac{\mathrm{Tr}\left(\mathcal{L}_{BCS,\alpha}c^\dagger_{\mathbf{k}\sigma}c_{\mathbf{k}\sigma}\right)}{\mathrm{Tr}\left(\rho_{0,\alpha}\right)} - n_{\mathbf{k}\sigma}\frac{\mathrm{Tr}\left(\mathcal{L}_{BCS,\alpha}\right)}{\mathrm{Tr}\left(\rho_{0,\alpha}\right)} \tag{51}$$

and

$$\partial_t \Delta_{\mathbf{k}} = \frac{\mathrm{Tr}\left(\mathcal{L}_{BCS,\alpha} c^\dagger_{\mathbf{k}\uparrow} c^\dagger_{-\mathbf{k}\downarrow}\right)}{\mathrm{Tr}\ (\rho_{0,\alpha})} - \Delta_{\mathbf{k}} \frac{\mathrm{Tr}\ (\mathcal{L}_{BCS,\alpha})}{\mathrm{Tr}\ (\rho_{0,\alpha})}, \quad (52)$$

where, in both equations, the second term comes from the normalization. In fact, one does not need to compute this normalization term as it is exactly canceled by the disconnected contractions coming from the trace in the first term. Let us consider the first term in Eq. (51). Due to the gaussianity of the state $\overline{\rho}_{0,\alpha} \equiv \rho_{0,\alpha}/\mathrm{Tr}\ (\rho_{0,\alpha})$, the trace is expressed in terms of all the possible contractions involving two fermionic lines. The contractions divide into two classes: the contractions that connect one operator of the Liouvillian and one operator from $c^\dagger_{\mathbf{k}\sigma} c_{\mathbf{k}\sigma}$ (connected contractions), and the contractions that connect operators belonging only to the Liouvillian or only to $c^\dagger_{\mathbf{k}\sigma} c_{\mathbf{k}\sigma}$ (disconnected contractions). It is easy to see that the sum of all the terms involving disconnected contractions cancels with the normalization term in the equations of motion. The same argument holds for Eq. (52). As a result, in order to take into account the normalization, we eliminate the second term and keep only the connected contractions in the first term

$$\partial_t n_{\mathbf{k}\sigma} = \mathrm{Tr}\ \left(\mathcal{L}_{BCS,\alpha}[\overline{\rho}_{0,\alpha}] c^\dagger_{\mathbf{k}\sigma} c_{\mathbf{k}\sigma}\right) \quad (53)$$

and

$$\partial_t \Delta_{\mathbf{k}} = \mathrm{Tr}\ \left(\mathcal{L}_{BCS,\alpha}[\overline{\rho}_{0,\alpha}] c^\dagger_{\mathbf{k}\uparrow} c^\dagger_{-\mathbf{k}\downarrow}\right), \quad (54)$$

where the lines indicate contraction connecting the Liouvillian and the operator.

The equations of motions can be written in terms of full Lindblad and hybrid, *i.e.* $\alpha < 1$, contributions as

$$\begin{aligned} \partial_t n_{\mathbf{k}\sigma} &= [\partial_t n_{\mathbf{k}\sigma}]_{\mathrm{Lindblad}} + (\alpha - 1)\,[\partial_t n_{\mathbf{k}\sigma}]_{\mathrm{hybrid}} \\ \partial_t \Delta_{\mathbf{k}\sigma} &= [\partial_t \Delta_{\mathbf{k}\sigma}]_{\mathrm{Lindblad}} + (\alpha - 1)\,[\partial_t \Delta_{\mathbf{k}\sigma}]_{\mathrm{hybrid}}, \end{aligned} \quad (55)$$

see appendix C for details. Upon defining the the complex gap amplitude as a function of both the loss and pump rates

$$\Phi \equiv [-|U| + i(\Gamma - P)]\,\Delta, \quad (56)$$

The full Lindbald contributions read

$$\begin{aligned} [\partial_t n_{\mathbf{k}\sigma}]_{\mathrm{Lindblad}} =& -2\mathrm{Im}\,[\Phi\Delta_{\mathbf{k}}] - \Gamma n n_{\mathbf{k}\sigma} \\ &+ 2P\left(1 - \frac{n}{2}\right)(1 - n_{\mathbf{k}\sigma}) \end{aligned} \quad (57)$$

and

$$\begin{aligned} [\partial_t \Delta_{\mathbf{k}}]_{\mathrm{Lindblad}} =& i2\epsilon_{\mathbf{k}}\Delta_{\mathbf{k}} - i\Phi(2n_{\mathbf{k}\sigma} - 1) - \Gamma n \Delta_{\mathbf{k}} \\ &- 2P\left(1 - \frac{n}{2}\right)\Delta_{\mathbf{k}}. \end{aligned} \quad (58)$$

The hybrid contributions further split into losses and pumps terms

$$\begin{aligned} [\partial_t n_{\mathbf{k}\sigma}]_{\mathrm{hybrid}} &= [\partial_t n_{\mathbf{k}\sigma}]^{\mathrm{loss}}_{\mathrm{hybrid}} + [\partial_t n_{\mathbf{k}\sigma}]^{\mathrm{pump}}_{\mathrm{hybrid}} \\ [\partial_t \Delta_{\mathbf{k}}]_{\mathrm{hybrid}} &= [\partial_t \Delta_{\mathbf{k}}]^{\mathrm{loss}}_{\mathrm{hybrid}} + [\partial_t \Delta_{\mathbf{k}}]^{\mathrm{pump}}_{\mathrm{hybrid}} \end{aligned} \quad (59)$$

where the each contribution reads

$$[\partial_t n_{\mathbf{k}\sigma}]^{\mathrm{loss}}_{\mathrm{hybrid}} = -\Gamma n \left[n^2_{\mathbf{k}\sigma} - |\Delta_{\mathbf{k}}|^2\right] + 2\Gamma\left[2\mathrm{Re}[\Delta\Delta^*_{\mathbf{k}}] n_{\mathbf{k}\sigma}\right], \quad (60)$$

$$\begin{aligned} [\partial_t n_{\mathbf{k}\sigma}]^{\mathrm{pump}}_{\mathrm{hybrid}} =& 2P\left(1 - \frac{n}{2}\right)\left[(1 - n_{\mathbf{k}\sigma})^2 - |\Delta_{\mathbf{k}}|^2\right] \\ &+ 2P\left[2\mathrm{Re}[\Delta\Delta^*_{\mathbf{k}}](1 - n_{\mathbf{k}\sigma})\right], \end{aligned} \quad (61)$$

$$[\partial_t \Delta_{\mathbf{k}}]^{\mathrm{loss}}_{\mathrm{hybrid}} = 2\Gamma\left[-n\Delta_{\mathbf{k}} n_{\mathbf{k}\sigma} + \Delta n^2_{\mathbf{k}\sigma} - \Delta^* \Delta^2_{\mathbf{k}}\right], \quad (62)$$

and

$$\begin{aligned} [\partial_t \Delta_{\mathbf{k}}]^{\mathrm{pump}}_{\mathrm{hybrid}} =& 2P\,(2 - n)\,\Delta_{\mathbf{k}}(n_{\mathbf{k}\sigma} - 1) + \\ &+ 2P\left[\Delta(1 - n_{\mathbf{k}\sigma})^2 - \Delta^*\Delta^2_{\mathbf{k}}\right]. \end{aligned} \quad (63)$$

We notice the loss contributions map into pumps upon the particle-hole transformation $n_{\mathbf{k}\sigma} \to 1 - n_{\mathbf{k}\sigma}$, and $\Delta_{\mathbf{k}} \to -\Delta^*_{\mathbf{k}}$.

V. RESULTS

In this section, we discuss the hybrid-dissipative dynamics obtained by solving the equations of motions for different quench protocols involving the sudden switch of the dissipation rates. In sections V A and V B we consider only two-body losses, whereas in section V C we consider the simultaneous action of pumps and losses.

A. Depletion dynamics with pair losses

We consider the sudden switch of the rate of the two-body losses $\Gamma(t) = \theta(t)\Gamma$ and set to zero the rate of the pumps $P = 0$. Due to the switching the two-particle loss, and in the absence of a counterbalancing pump mechanism, the system is expect to naturally evolve towards the zero density limit. In Fig. 1, we show the depletion dynamics of the density and the superconducting order parameter amplitude for a fixed values $|U|/W = 1.0$ and $\Gamma/|U| = 0.08$ and different values of the hybrid parameter α from the Lindblad ($\alpha = 1$, yellow lines) to the non-Hermitian ($\alpha = 0$, dark purple lines) limits.

In the Lindblad limit, the decay of both quantities shows an exponential decay at short times, followed by universal power-laws $|\Delta(t)| \sim t^{-2}$ and $n(t) \sim t^{-1}$. As discussed in Ref. 52, the power-law decay of the density is characteristic of the many-body nature of the jump operators which give rise to effective single-particle losses whose rates are proportional to the density, see Eqs. (57)-(58). In particular, the rates becomes smaller and smaller as the density decreases effectively slowing down the depletion of the system. Both dynamics can be understood by looking at the equations of motions for density and order parameter amplitude for $\alpha = 1$

$$\partial_t n_{\alpha=1} = -4\Gamma|\Delta|^2 - \Gamma n^2, \quad (64)$$

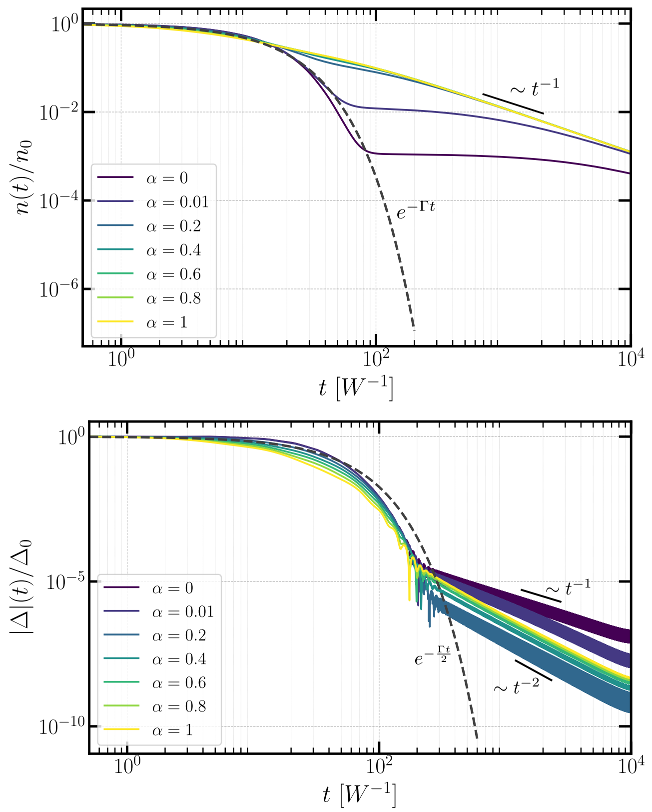

Figure 1. Dynamics of the particles density (top panel) and the superconducting order parameter amplitude (bottom panel) for the different values of the parameter α. $|U|/W = 1.0$, $\Gamma/|U| = 0.08$ and $P/|U| = 0.0$.

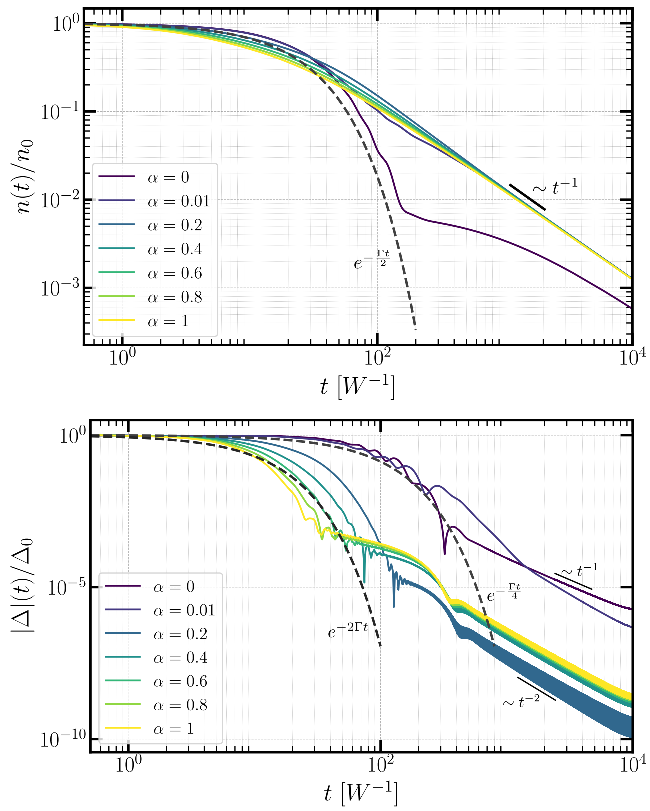

Figure 2. Dynamics of the particles density (top panel) and the superconducting order parameter amplitude (bottom panel) for the different values of the parameter α. $|U|/W = 0.5$, $\Gamma/|U| = 0.08$ and $P/|U| = 0.0$.

and

$$\partial_t|\Delta|^2_{\alpha=1} = -2\Gamma|\Delta|^2 + 2i\sum_{\mathbf{k}\mathbf{k}'}(\epsilon_{\mathbf{k}} - \epsilon_{\mathbf{k}'})\Delta_{\mathbf{k}}\Delta^*_{\mathbf{k}'}. \tag{65}$$

The equation of motion for the density has a term proportional to the order parameter amplitude, which describes the particle depletion due to the loss of particles in the condensate, and a term $\sim -\Gamma n^2$ which comes from the effective single-particle losses and takes into account losses of particles outside the condensate. At long times, one can neglect the contribution of the order parameter, and the equation of motion reduces to $\partial_t n \sim -\Gamma n^2$ giving rise to $n(t) \sim \frac{n_0}{(1+\Gamma t)}$.

The dynamics of the order parameter amplitude is characterized by the competition between the exponential decay and a dephasing term which depends on the dynamics of the pair amplitudes for each mode. The exponential decay is the dominant contribution at short times. At long times, when $|\Delta|/\Delta_0 \ll 1$, the exponential term can be neglected so that the dephasing becomes the dominant mechanism $\partial_t|\Delta|^2_{\alpha=1} \sim 2i\sum_{\mathbf{k}\mathbf{k}'}(\epsilon_{\mathbf{k}} - \epsilon_{\mathbf{k}'})\Delta_{\mathbf{k}}\Delta^*_{\mathbf{k}'}$. The $\sim t^{-2}$ decay can be understood by considering the equations of motions for each paring amplitude $\Delta_{\mathbf{k}}$. Upon neglecting contributions from the average pairing amplitude, we obtain $\Delta_{\mathbf{k}} \sim e^{i2\epsilon_{\mathbf{k}}t}/(1+\Gamma t)$, where the $(1+\Gamma t)$ denominator comes from the power-law decay of the density. This shows that the $\sim t^{-2}$ decay in $\Delta = \sum_{\mathbf{k}}\Delta_{\mathbf{k}}$ has a $\sim t^{-1}$ contribution coming from the density, and an additional $\sim t^{-1}$ contribution from the momentum summation of the oscillatory terms with phases that accumulate proportionally to $\epsilon_{\mathbf{k}}$ for each mode. We also notice that the dephasing term acts non-trivially on the exponential decay at short times. Indeed, the exponential term alone in the equation (65) would predict a simple $|\Delta| \sim e^{-\Gamma t}$ decay rate, independent on the interaction strength $|U|$. However, as can be appreciated by comparing Fig. 1 with Fig. 2, showing the depletion dynamics for a different value of $|U|/W = 0.5$, we find that the short times exponential decay evolves as a function of $|U|$. While the interaction strength $|U|$ does not explicitly enter in the exponential decay term of Eq. (65), it does enters the dynamics of the phase of the pairing amplitude signaling a non-negligible contribution of dephasing also at short times.

Moving away from the Lindblad limit, $\alpha < 1$, we observe a dynamics similar to the Lindblad one occurring on longer time scales. In particular, as α is decreased, the exponential decay becomes slower, and the transition towards the power-law regime gets delayed. Physically, this is expected since decreasing α is interpreted as an ef-

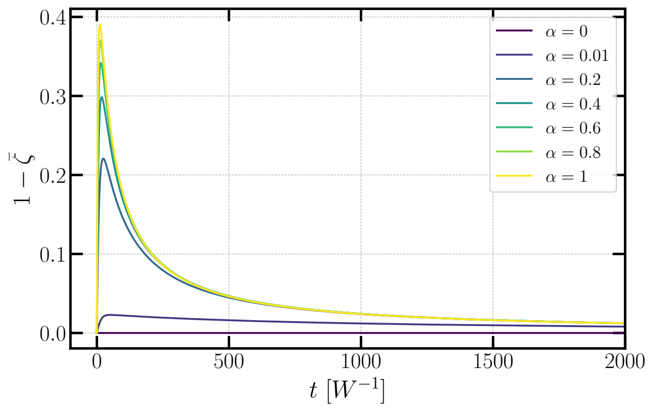

Figure 3. Dynamics of the pseudospin length for the different values of the parameter α. $U/W = 1.0$, $\Gamma/|U| = 0.08$ and $P/|U| = 0.0$.

fective suppression of the dissipative channels due to the post-selection of quantum trajectories with reduced number of jumps. Remarkably, approaching the NH limit, $\alpha \to 0$, the dynamics sharply changes.

In the purely NH limit, $\alpha = 0$, the density displays an exponential decay for an extended interval of time. After that, we observe the formation of a quasi-steady state characterized by a density plateau. Eventually, the dynamics slowly recovers the t^{-1} decay for $tW \gg 1$. At the same time, the power-law decay of the order parameter suddenly changes from the $\sim t^{-2}$ to a $\sim t^{-1}$ decay. For infinitesimal α, of the order of $\alpha \lesssim 0.01$, the dynamics interpolates between the NH and the Lindblad limits. The same qualitative dynamics, with a much less pronounced quasi-steady state density plateau, is observed for $|U|/W = 0.5$. By comparing the dynamics of the density and the order parameter for $\alpha = 0$, we see that, the NH dynamics, as compared to the Lindblad one, is characterized by a faster depletion of particles and a slower decay of the order parameter amplitude.

To get an insight on the above dynamics, we explicitly write the equation of motion for the density for arbitrary α

$$\partial_t n_\alpha = -4\Gamma|\Delta|^2 - \Gamma n^2 + 2(\alpha-1)\Gamma\times \\ \times \sum_{\mathbf{k}\sigma}\left[\frac{n}{2}\left(|\Delta_{\mathbf{k}}|^2 - n_{\mathbf{k}\sigma}^2\right) - 2\mathrm{Re}(\Delta\Delta_{\mathbf{k}}^*)n_{\mathbf{k}\sigma}\right]. \tag{66}$$

In equation (66), the first two terms correspond to the Lindbald dynamics, see Eq. (64), whereas the last term is the correction due the hybrid nature of the Liouvillian. To make progress, we analyze the equation of motions for the density in combination with the dynamics of the pseudospin length, defined as

$$\zeta_{\mathbf{k}} \equiv \sum_{i=x,y,z}\left[\sigma_{\mathbf{k}}^i\right]^2 \tag{67}$$

with $\sigma_{\mathbf{k}}^x = 2\mathrm{Re}\Delta_{\mathbf{k}}$, $\sigma_{\mathbf{k}}^y = 2\mathrm{Im}\Delta_{\mathbf{k}}$ and $\sigma_{\mathbf{k}}^z = 2n_{\mathbf{k}\sigma} - 1$. In the equilibrium BCS state, $\zeta_{\mathbf{k}} = 1$ for each mode. Upon switching-on two-particle losses, the pseudo-spin length deviates from the equilibrium value, $\zeta_{\mathbf{k}} = 1$, and recovers at long times its initial value when the system approaches the vacuum state characterized by $\sigma_{\mathbf{k}}^x = \sigma_{\mathbf{k}}^y = 0$, and $\sigma_{\mathbf{k}}^z = -1$. The evolution of the $\zeta_{\mathbf{k}}$ is governed by the equation

$$\partial_t\zeta_{\mathbf{k},\alpha} = -C_{\mathbf{k}\alpha}(\zeta_{\mathbf{k}} - 1) - \alpha\Gamma n n_{\mathbf{k}\sigma} \tag{68}$$

with $C_{\mathbf{k}\alpha} \equiv -2\Gamma n + (\alpha - 1)\left[4\mathrm{Re}(\Delta\Delta_{\mathbf{k}}^*) + n(2n_{\mathbf{k}\sigma} + 1)\right]$. From Eq. (68), we see that, while for $\alpha = 1$ the pseudo-spin length evolves accordingly to $\partial_t\zeta_{\mathbf{k}} = -2\Gamma n(\zeta_{\mathbf{k}} - 1) - \Gamma n n_{\mathbf{k}}$, for $\alpha = 0$ the initial pseudo-spin length $\zeta_{\mathbf{k}}$ becomes a constant of motion. The conservation of the pseudo-spin length in the NH limit is shown in Fig. 3, where we report the evolution of the average pseudo-spin length $\bar{\zeta} = \sum_{\mathbf{k}} \bar{\zeta}_{\mathbf{k}}$ for different values of α.

The conservation of the pseudo-spin implies that the pairing amplitude and the occupation of each mode are constrained by the relation

$$|\Delta_{\mathbf{k}}|^2 = n_{\mathbf{k}\sigma}\left(1 - n_{\mathbf{k}\sigma}\right). \tag{69}$$

We can now exploit the conservation of the pseudospin length and use Eq. (69) to rewrite the equation of motion for the density for $\alpha = 0$ as

$$\partial n_{\alpha=0} = -4\Gamma|\Delta|^2 - 4\Gamma n\sum_{\mathbf{k}}|\Delta_{\mathbf{k}}|^2 + 4\Gamma\sum_{\mathbf{k}} n_{\mathbf{k}}\mathrm{Re}(\Delta\Delta_{\mathbf{k}}^*). \tag{70}$$

Similar manipulations for the equation of motions of the order parameter amplitude leads to

$$\partial_t|\Delta|_{\alpha=0}^2 \sim -2\Gamma|\Delta|^2 + 2i\sum_{\mathbf{k}\mathbf{k}'}(\epsilon_{\mathbf{k}} - \epsilon_{\mathbf{k}'})\Delta_{\mathbf{k}}\Delta_{\mathbf{k}'}^* + 8\Gamma|\Delta|^4, \tag{71}$$

where we neglected subleading corrections and the quartic term must be understood as an order of magnitude estimate coming from the approximation $(\Delta^*)^2\sum_{\mathbf{k}}\Delta_{\mathbf{k}}^2 \sim |\Delta|^2\sum_{\mathbf{k}}|\Delta_{\mathbf{k}}|^2 \sim |\Delta|^4$.

Eq. (71) reveals that the dynamics of the order parameter amplitude is essentially the same of the Lindblad case, with an exponential decay and a dephasing term. The only difference is in the $\sim 8\Gamma|\Delta|^4$ term which partially counterbalances the exponential term and is likely to be responsible of the slower decay of $|\Delta|$ upon decreasing α. The power-law decay at long-times has the same dephasing origin as in the Lindblad case. However, the exponent changes from t^{-2} to t^{-1} due to the fact that the additional $\sim t^{-1}$ contribution coming from the power-law decay of the density is now suppressed.

Considering the equation of motion for the density, we observe that, as a consequence of the pseudo-spin conservation, the $-\Gamma n^2$ terms that was describing effective single particle losses and was responsible of the power law decay of the density for $\alpha > 0$, disappears in the NH limit. This means that, effective single particle losses are suppressed in the NH limit, and the depletion of particle is completely dragged by the decay of the order parameter. At short times, the last two terms in Eq. (70) approximately cancels each other, so that we can approximate

$\partial_t n_{\alpha=0} \sim -4\Gamma|\Delta|^2$. By assuming a simple exponential decay with rate γ (which depends itself on the dissipation rate Γ) for the order parameter $|\Delta| \sim |\Delta_0| e^{-\gamma t}$, we obtain $n_{\alpha=0} \sim n_0 + \frac{2\Gamma}{\gamma}|\Delta_0|^2 \left(e^{-2\gamma t} - 1\right)$ which implies that, eventually, a plateau is expected for $\gamma t \gg 1$. The value of the plateau density depends on the actual dynamics of the order parameter amplitude that, as can be appreciated from the reference exponential decays in the figures, is richer than the simple decay used in this argument. Nonetheless, we observe that the above argument is further supported by the fact that, in the numerics, the exponential decay rate of the density is found to be roughly twice the decay rate of the order parameter amplitude.

At long times, we can assume that, due to dephasing, $|\sum_{\mathbf{k}} \Delta_{\mathbf{k}}| \ll \sum_{\mathbf{k}} |\Delta_{\mathbf{k}}|$ and retain only the second term in Eq. (70). This leads to $\partial_t n_{\alpha=0} \sim -4\Gamma n \sum_{\mathbf{k}} |\Delta_{\mathbf{k}}|^2 = -\Gamma n \sum_{\mathbf{k}} 2n_{\mathbf{k}} - n_{\mathbf{k}}^2$ where, in the last step, we used again the pseudo-spin length conservation. For very long-times $n_{\mathbf{k}}^2 \ll n_{\mathbf{k}}$ and the dynamics reduces to $\partial_t n_{\alpha=0} \sim -2\Gamma n^2$ which justifies the $\sim t^{-1}$ decay of the density for $tW \gg 1$. Despite the apparent similarity between such a long-time power-law decay of the density for $\alpha = 0$ and the same power-law decay for $\alpha = 1$, we stress that the two behaviors have completely different origin. In the latter case, $\alpha = 1$, the power-law decay is due to the effective single-particle losses and it characterizes the dynamics at all times. On the contrary, for $\alpha = 0$, effective single-particle losses are suppressed and the power-law decay emerges only at long times when the dephasing decay of the order parameter becomes the dominant contribution.

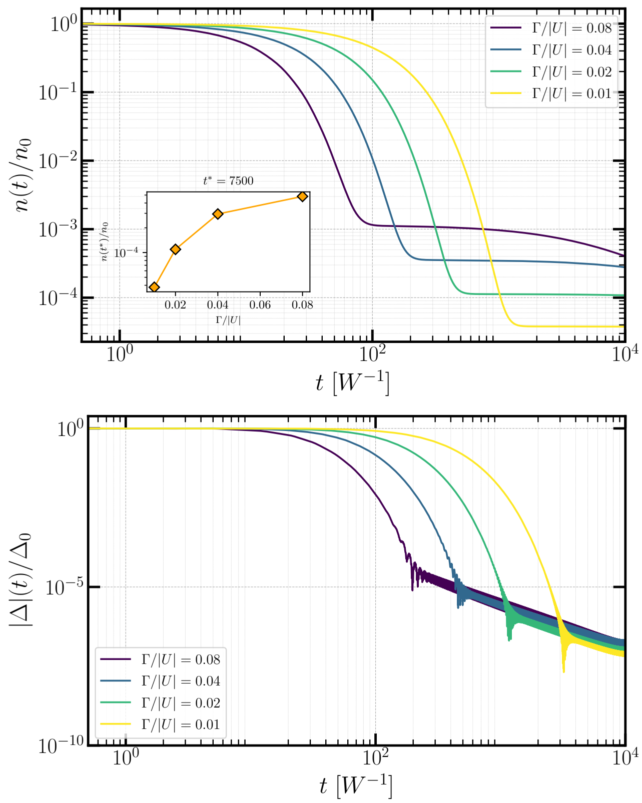

Figure 4. Dynamics of the particle density (top panel) and the superconducting order parameter amplitude (bottom panel) in the NH limit for different values of the dissipation rate Γ. $|U|/W = 1.0$, $\alpha = 0$ and $P/|U| = 0.0$. Inset in the top panel: density in the quasi-steady plateau as a function of the dissipation rate.

B. Non-Hermitian Zeno Effect

We now discuss the direct consequences of the dynamics in the NH limit described in the previous section. In the NH limit, the pseudospin length conservation suppresses effective single particle losses and the decay of density is completely tied to the decay of the order parameter. This leads to an exponential decay at short times ending up in a plateau which slowly recovers the power-law decay $\sim t^{-1}$ at later times due to the dephasing of the order parameter. This behaviour has interesting consequences. First of all, the onset of the $\sim t^{-1}$ decay is expected to occur earlier the faster the decay of the order parameter. Moreover, the faster the decay of the order parameter, the smaller the number of particles that can be depleted before the plateau set in. In other words, as already observed in Figs. 1-2, the slower the decay of the order parameter the more effective the depletion of particles due to NH two-body losses. These observations point towards a Non-Hermitian Zeno (NHZ) effect [77–82] in which, before the power-law decay due to dephasing sets in, the density plateau in the quasi-steady state increases as a function of Γ. In Fig. 4, we report evidence of such a NHZ effect by showing the NH dynamics of the density and superconducting order parameter amplitude for several values of the dissipation rate Γ. As it is clear from the inset, the plateau density increases as function of the decay rate. Analogously, we observe that the smaller the Γ the smaller the amplitude of the order parameter reached after the exponential decay.

C. Driven-dissipative dynamics with pair losses and pumps

We now consider the driven-dissipative case in which both two-body losses and pumps are simultaneously switched-on. We consider the equally balanced case $\Gamma = P$ which preserves particle-hole symmetry so that the density remains constant in time $n(t) = 1$. Due to the homogeneous rates of pairs injection and pairs removal, the system is expected to continuously absorb energy and the order parameter is expected to decay until an infinite temperature state is eventually reached. In Fig. 5, we show the dynamics of the order parameter for fixed value of the dissipation rate and various hybrid parameters α from the Lindbald, $\alpha = 1$, to the NH, $\alpha = 0$, limits. Starting from $\alpha = 1$, we see that in the driven-dissipative

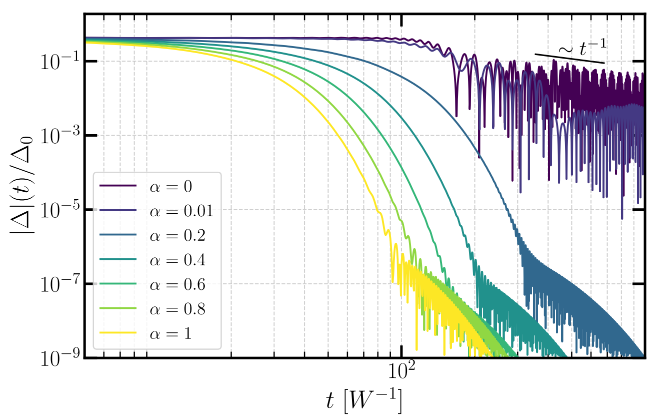

Figure 5. Dynamics of the order parameter with simultaneous pair pumps and losses for different values of the parameter α. $|U|/W = 1.0$ and $\Gamma/|U| = P/|U| = 0.08$.

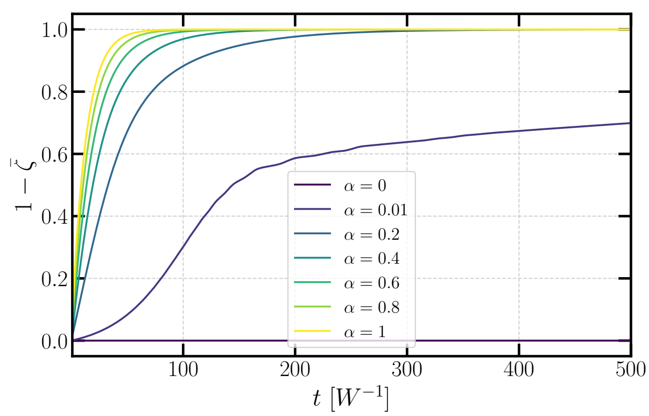

Figure 7. Dynamics of the average pseudo-spin length for different values of α. $|U|/W = 1.0$ and $\Gamma/|U| = P/|U| = 0.08$.

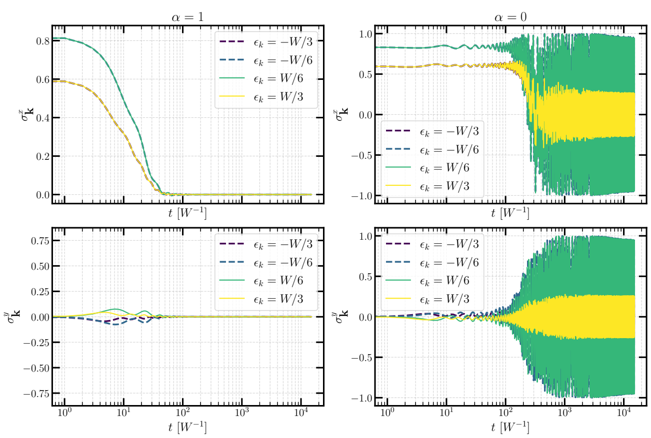

Figure 6. Dynamics of the pairing amplitudes $\sigma^x_{\mathbf{k}}$ (top panels) and $\sigma^y_{\mathbf{k}}$ (bottom panels) for $\alpha = 1$ (left panels) and $\alpha = 0$ (right panels) for selected modes above and below the Fermi level. $|U|/W = 1.0$ and $\Gamma/|U| = P/|U| = 0.08$.

case the decay of the order parameter has always an exponential character. This is expected as, in contrast to the previous case, the dissipation rates for the effective single-particle dissipators, namely $n\Gamma$ for the losses and $(2-n)P$ for the pumps, remain constant in time. As α is decreased, the exponential decay becomes slower, as expected by the effective reduction of the effects of the jump operator. The dynamics smoothly evolves as a function of α until, similarly to what discussed for the only loss case, it sharply changes approaching the NH limit. For $\alpha = 0$, the order parameter amplitude remains more ore less constant for an extended interval of time until a rapidly oscillating power-law decay $\sim t^{-1}$ sets in for $tW \gtrsim 100$.

The power-law decay of the order parameter suggests that, in the NH limit, the dynamics is governed by a purely dephasing mechanism. In contrast, in the Lindblad limit, the exponential decay indicates the decay of the pairing amplitude of each mode. This is clearly seen in Fig. 6, where we report the dynamics of $\sigma^x_{\mathbf{k}}$ and $\sigma^y_{\mathbf{k}}$ for representative modes at selected energies above and below the Fermi energy. We observe that, for $\alpha = 1$, the pairing amplitudes of the single modes all decay to zero. In contrast, for $\alpha = 0$, these quantities oscillate with constant amplitude, thus showing that the fast oscillating power-law decay of Fig. 5 is completely governed by the destructive interference among the different modes.

To understand the origin of such a sharp difference between the dynamics in the Lindblad and NH limits, we resort once again to the dynamics of the pseudo-spin length $\zeta_{\mathbf{k}}$. Analogously to the case of only losses, the NH dynamics preserves the pseudo-spin length, see Fig. 7. It is straightforward to see that the conservation of the pseudo-spin length hinders the decay to zero of the pairing amplitudes of the single modes. Indeed, if $\sigma^x_{\mathbf{k}} = \sigma^y_{\mathbf{k}} = 0$ the pseudo-spin conservation would require $\sigma^z_{\mathbf{k}} = \pm 1$. Such a pseudo-spin configuration can be realized only for the completely filled or completely empty states that, due to the perfect balance between pair pumps and losses, can never be reached. On the contrary, due to the unconstrained evolution of the pseudo-spin length, the $\sigma^x_{\mathbf{k}} = \sigma^x_{\mathbf{k}} = 0$ state can always be reached within the Lindblad dynamics.

The above observations show that the Lindblad and the NH driven-dissipative dynamics are characterized by the distinct steady states. To fully characterize the steady states reached by the different non-unitary dynamics, we plot in Fig. 8 the occupation number $n_{\mathbf{k}\sigma} = \frac{1+\sigma^z_{\mathbf{k}}}{2}$ for selected modes above and before the Fermi level. In the Lindblad limit, the dynamics converges towards the infinite temperature state with homogeneous occupation for all modes $n_{\mathbf{k}\sigma} = \frac{1}{2}$ or, equivalently, $\sigma^z_{\mathbf{k}} = 0$. The same occurs for the hybrid dynamics with $\alpha < 1$. On the contrary, in the NH limit, we observe that the occupations of the modes are characterized by a strongly oscillating dynamics. Interestingly, after a certain time, the strong oscillations leads to a population inversion with states below the Fermi energy becoming less populated than the

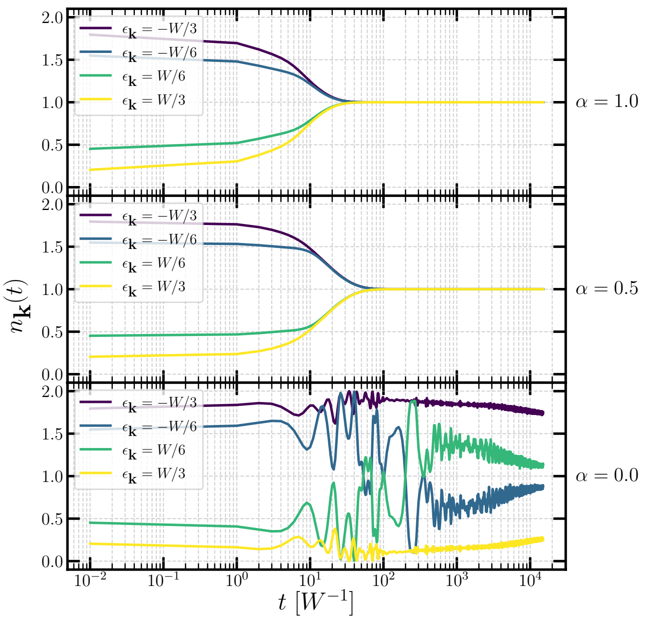

Figure 8. Dynamics of the occupation numbers for selected modes above and below the Fermi level for $\alpha = 1.0$ (top), $\alpha = 0.5$ (middle) and $\alpha = 0.0$ (bottom). $|U|/W = 1.0$ and $\Gamma/|U| = P/|U| = 0.08$.

states above. This shows how in the NH limit the system skips the infinite temperature steady states and evolves towards a highly non-equilibrium steady state akin to a negative temperature state.

VI. CONCLUSIONS

We discussed the non-unitary dynamics of dissipative fermions described by a hybrid Lindblad evolution, interpolating between the full unconditional Lindblad dynamics and the full post-selection of quantum jump trajectories captured by the no-click NH dynamics. By tuning the control parameter α, between $\alpha = 0$ (NH dynamics) and $\alpha = 1$ (Lindblad) we investigate the role of quantum jumps on the dynamics of the density matrix. To tackle the problem, we have introduced time-dependent variational principles based on actions defined for arbitrary values of α. The variational principles naturally take into account the state normalization in the hybrid Lindbladian evolution and, in the NH limit $\alpha = 0$, reduce to an extended Dirack-Frenkel for NHH.

We have applied the variational principles to the dynamics of driven-dissipative BCS superconductors described by an attractive Hubbard model in the presence of two-body losses, and in the simultaneous presence of both, equally balanced, two-body losses and pumps. In the first case, the non-unitary dynamics leads to the complete depletion of the system, whereas in the driven-dissipative case the non-unitary dynamics with perfectly balanced pumps and losses leads to the formation of non-trivial steady-states.

By considering the above non equilibrium protocols, we explored the evolution of the non-unitary dynamics from the Lindblad, $\alpha = 1$, to the NH limits, $\alpha = 0$. In all the discussed cases, we showed how the quantum jumps play a crucial for the non-unitary dynamics. Starting from $\alpha = 1$, we progressively reduce the relative weight of the quantum jumps, $\alpha < 1$, and show how the non-unitary dynamics is equivalent to a Lindblad dynamics occurring on longer time scales. This suggests that the suppression of the relative weight of the quantum jumps can be understood as an effective reduction of the dissipation rate. In contrast, in the no-click limit, $\alpha = 0$, when the quantum jumps are completely neglected, we observe sharp qualitative changes in the dynamics for what concerns both the evolution towards the steady state, and the properties of the steady state. We show that such a sharp qualitative changes in the non-unitary dynamics are due to the an exact conservation of the pseudospin length occurring for $\alpha = 0$. In the case of the depletion dynamics, the pseudospin length conservation determines the suppression of the effective single-particle losses so that the decay of the density becomes completely tied to the decay of the order parameter. For the driven-dissipative case, the same conservation hinders the exponential decay of the order parameter leading to a purely dephasing dynamics characterized by a slow power-law of the order parameter.

By analysing the dynamics in different regimes, we showed that the NH dynamics leads to non-trivial steady states that cannot be reached in the presence of quantum jumps. For the depletion dynamics, our results show that the evolution towards the vacuum state occurs through a quasi-steady state characterized by a density plateau. The particle suppression is the more effective the faster the decay of the order parameter, leading to the emergence of a Non-Hermitian Zeno effect characterized by quasi-steady states with density increasing as a function of the dissipation rate. For the driven-dissipative case, our results show that the the NH dynamics drives the systems towards the a highly non-equilibrium steady state with population inversion.

ACKNOWLEDGMENTS

G.M. acknowledges support by the MUR Italian Minister of Research through a "Rita-Levi Montalcini" fellowship. M.S. acknowledges financial support from the ERC consolidator Grant No. 101002955 - CONQUER.

[1] V. Weisskopf and E. Wigner, Zeitschrift für Physik **63**, 54 (1930).
[2] R. K. Wangsness and F. Bloch, Phys. Rev. **89**, 728 (1953).
[3] H. P. Breuer and F. Petruccione, *The Theory of Open Quantum Systems*, 1st ed., Vol. 9780199213 (OUP Oxford, 2007).
[4] R. Fazio, J. Keeling, L. Mazza, and M. Schirò, "Many-body open quantum systems," (2025), arXiv:2409.10300 [quant-ph].
[5] R. Trivedi, A. Franco Rubio, and J. I. Cirac, Nature Communications **15**, 6507 (2024).
[6] L. Lin, "Dissipative preparation of many-body quantum states: Towards practical quantum advantage," (2025), arXiv:2505.21308 [quant-ph].
[7] G. Lindblad, Communications in Mathematical Physics **48**, 119 (1976).
[8] C. Gardiner and P. Zoller, *Quantum Noise*, 3rd ed. (Springer Berlin, 2004).
[9] J. Dalibard, Y. Castin, and K. Molmer, Phys. Rev. Lett. **68**, 580 (1992).
[10] M. B. Plenio and P. L. Knight, Rev. Mod. Phys. **70**, 101 (1998).
[11] H. M. Wiseman and G. J. Milburn, *Quantum Measurement and Control* (Cambridge University Press, Cambridge, England, 2009).
[12] Z. G. Yuto Ashida and M. Ueda, Advances in Physics **69**, 249 (2020), https://doi.org/10.1080/00018732.2021.1876991.
[13] T. E. Lee and C.-K. Chan, Phys. Rev. X **4**, 041001 (2014).
[14] T. E. Lee, F. Reiter, and N. Moiseyev, Phys. Rev. Lett. **113**, 250401 (2014).
[15] T. E. Lee, Phys. Rev. Lett. **116**, 133903 (2016).
[16] M. Nakagawa, N. Kawakami, and M. Ueda, Phys. Rev. Lett. **121**, 203001 (2018).
[17] A. Biella and M. Schiró, Quantum **5**, 528 (2021).
[18] S. Gopalakrishnan and M. J. Gullans, Phys. Rev. Lett. **126**, 170503 (2021).
[19] K. Yamamoto, M. Nakagawa, M. Tezuka, M. Ueda, and N. Kawakami, Phys. Rev. B **105**, 205125 (2022).
[20] S.-X. Hu, Y. Fu, and Y. Zhang, Phys. Rev. B **108**, 245114 (2023).
[21] Y. L. Gal, X. Turkeshi, and M. Schirò, SciPost Phys. **14**, 138 (2023).
[22] X. Turkeshi and M. Schiró, Phys. Rev. B **107**, L020403 (2023).
[23] V. Meden, L. Grunwald, and D. M. Kennes, Reports on Progress in Physics **86**, 124501 (2023).
[24] X.-J. Yu, Z. Pan, L. Xu, and Z.-X. Li, Phys. Rev. Lett. **132**, 116503 (2024).
[25] R. D. Soares and M. Schirò, SciPost Phys. **17**, 128 (2024).
[26] R. D. Soares, Y. L. Gal, C. Y. Leung, D. Meidan, A. Romito, and M. Schirò, "Symmetries, conservation laws and entanglement in non-hermitian fermionic lattices," (2025), arXiv:2504.08557 [cond-mat.stat-mech].
[27] F. Minganti, A. Miranowicz, R. W. Chhajlany, I. I. Arkhipov, and F. Nori, Phys. Rev. A **101**, 062112 (2020).
[28] J. P. Garrahan and I. Lesanovsky, Phys. Rev. Lett. **104**, 160601 (2010).
[29] S. Gupta, H. K. Yadalam, M. Kulkarni, and C. Aron, Phys. Rev. A **109**, L050201 (2024).
[30] Y. Le Gal, X. Turkeshi, and M. Schirò, PRX Quantum **5**, 030329 (2024).
[31] H. Weimer, A. Kshetrimayum, and R. Orús, Rev. Mod. Phys. **93**, 015008 (2021).
[32] L. M. Sieberer, M. Buchhold, and S. Diehl, Reports on Progress in Physics **79**, 096001 (2016).
[33] J. Cui, J. I. Cirac, and M. C. Bañuls, Phys. Rev. Lett. **114**, 220601 (2015).
[34] H. Landa, M. Schiró, and G. Misguich, Phys. Rev. Lett. **124**, 043601 (2020).
[35] D. Kilda, A. Biella, M. Schirò, R. Fazio, and J. Keeling, SciPost Phys. Core **4**, 005 (2021).
[36] C. Mc Keever and M. H. Szymańska, Phys. Rev. X **11**, 021035 (2021).
[37] L. Shirizly, G. Misguich, and H. Landa, Phys. Rev. Lett. **132**, 010601 (2024).
[38] A. J. Daley, Advances in Physics **63**, 77 (2014).
[39] A. Sander, M. Fröhlich, M. Eigel, J. Eisert, P. Gelß, M. Hintermüller, R. M. Milbradt, R. Wille, and C. B. Mendl, "Large-scale stochastic simulation of open quantum systems," (2025), arXiv:2501.17913 [quant-ph].
[40] P. Deuar, A. Ferrier, M. Matuszewski, G. Orso, and M. H. Szymanska, PRX Quantum **2**, 010319 (2021).
[41] K. Nagao, Y. Takasu, Y. Takahashi, and I. Danshita, Phys. Rev. Res. **3**, 043091 (2021).
[42] D. A. Hryniuk and M. H. Szymańska, Quantum **8**, 1475 (2024).
[43] F. Vicentini, A. Biella, N. Regnault, and C. Ciuti, Phys. Rev. Lett. **122**, 250503 (2019).
[44] A. Nagy and V. Savona, Phys. Rev. Lett. **122**, 250501 (2019).
[45] D. Luo, Z. Chen, J. Carrasquilla, and B. K. Clark, Phys. Rev. Lett. **128**, 090501 (2022).
[46] M. Schiró and M. Fabrizio, Phys. Rev. Lett. **105**, 076401 (2010).
[47] M. Fabrizio, in *New Materials for Thermoelectric Applications: Theory and Experiment*, edited by V. Zlatic and A. Hewson (Springer Netherlands, Dordrecht, 2013) pp. 247–273.
[48] G. Mazza, A. Amaricci, M. Capone, and M. Fabrizio, Phys. Rev. B **91**, 195124 (2015).
[49] G. Mazza, M. Gandolfi, M. Capone, F. Banfi, and C. Giannetti, Nature Communications **12**, 6904 (2021).
[50] H. Weimer, Phys. Rev. Lett. **114**, 040402 (2015).
[51] D. Eeltink, F. Vicentini, and V. Savona, "Variational dynamics of open quantum systems in phase space," (2023), arXiv:2307.07429 [quant-ph].
[52] G. Mazza and M. Schirò, Phys. Rev. A **107**, L051301 (2023).
[53] Y.-F. Qu, M. Stefanini, T. Shi, T. Esslinger, S. Gopalakrishnan, J. Marino, and E. Demler, Phys. Rev. B **111**, 155113 (2025).
[54] K. Yamamoto, M. Nakagawa, N. Tsuji, M. Ueda, and N. Kawakami, Phys. Rev. Lett. **127**, 055301 (2021).
[55] K. Yamamoto, M. Nakagawa, K. Adachi, K. Takasan, M. Ueda, and N. Kawakami, Phys. Rev. Lett. **123**, 123601 (2019).
[56] A. Nava, C. A. Perroni, R. Egger, L. Lepori, and D. Giuliano, Phys. Rev. B **108**, 245129 (2023).
[57] A. Nava, C. A. Perroni, R. Egger, L. Lepori, and D. Giuliano, Phys. Rev. B **109**, L041107 (2024).

[58] K. Honda, S. Taie, Y. Takasu, N. Nishizawa, M. Nakagawa, and Y. Takahashi, Phys. Rev. Lett. **130**, 063001 (2023).
[59] D. J. Young, A. Chu, E. Y. Song, D. Barberena, D. Wellnitz, Z. Niu, V. M. Schäfer, R. J. Lewis-Swan, A. M. Rey, and J. K. Thompson, Nature **625**, 679 (2024).
[60] A. Dorda, M. Nuss, W. von der Linden, and E. Arrigoni, Phys. Rev. B **89**, 165105 (2014).
[61] M. Vanhoecke and M. Schirò, Phys. Rev. B **109**, 125125 (2024).
[62] T. Bourdel, L. Khaykovich, J. Cubizolles, J. Zhang, F. Chevy, M. Teichmann, L. Tarruell, S. J. J. M. F. Kokkelmans, and C. Salomon, Phys. Rev. Lett. **93**, 050401 (2004).
[63] Q. Chen, J. Stajic, S. Tan, and K. Levin, Physics Reports **412**, 1 (2005).
[64] H. Biss, L. Sobirey, N. Luick, M. Bohlen, J. J. Kinnunen, G. M. Bruun, T. Lompe, and H. Moritz, Phys. Rev. Lett. **128**, 100401 (2022).
[65] A. Toschi, M. Capone, and C. Castellani, Phys. Rev. B **72**, 235118 (2005).
[66] G. Mazza, A. Amaricci, and M. Capone, Phys. Rev. B **103**, 094514 (2021).
[67] R. A. Barankov, L. S. Levitov, and B. Z. Spivak, Phys. Rev. Lett. **93**, 160401 (2004).
[68] R. A. Barankov and L. S. Levitov, Phys. Rev. Lett. **96**, 230403 (2006).
[69] E. A. Yuzbashyan, B. L. Altshuler, V. B. Kuznetsov, and V. Z. Enolskii, Phys. Rev. B **72**, 220503 (2005).
[70] E. A. Yuzbashyan, O. Tsyplyatyev, and B. L. Altshuler, Phys. Rev. Lett. **96**, 097005 (2006).
[71] G. Mazza, Phys. Rev. B **96**, 205110 (2017).
[72] G. Seibold and J. Lorenzana, Phys. Rev. B **102**, 144502 (2020).
[73] H. P. Ojeda Collado, G. Usaj, J. Lorenzana, and C. A. Balseiro, Phys. Rev. B **99**, 174509 (2019).
[74] G. Mazza and M. Fabrizio, Phys. Rev. B **86**, 184303 (2012).
[75] G. Seibold, C. Castellani, and J. Lorenzana, Phys. Rev. B **105**, 184513 (2022).
[76] H. P. O. Collado, N. Defenu, and J. Lorenzana, "Engineering higgs dynamics by spectral singularities," (2022).
[77] N. Syassen, D. M. Bauer, M. Lettner, T. Volz, D. Dietze, J. J. García-Ripoll, J. I. Cirac, G. Rempe, and S. Dürr, Science **320**, 1329 (2008).
[78] J. J. García-Ripoll, S. Dürr, N. Syassen, D. M. Bauer, M. Lettner, G. Rempe, and J. I. Cirac, New Journal of Physics **11**, 013053 (2009).
[79] H. Fröml, A. Chiocchetta, C. Kollath, and S. Diehl, Physical Review Letters **122**, 040402 (2019).
[80] A. Biella and M. Schiró, Quantum **5**, 528 (2021).
[81] D. Rossini, A. Ghermaoui, M. B. Aguilera, R. Vatré, R. Bouganne, J. Beugnon, F. Gerbier, and L. Mazza, Physical Review A **103**, L060201 (2021).
[82] O. Scarlatella, A. A. Clerk, R. Fazio, and M. Schiró, Physical Review X **11**, 031018 (2021).

Appendix A: Hybrid DMVP with Gaussian states

In this section we report details of the application of the DMVP to Gaussian states discussed in Sec. III. We start from the case $\alpha = 1$. For this, we need to compute the trace

$$\mathrm{Tr}\,(\rho_{\mathrm{aux}}\mathcal{L}_1[\rho_0]) = -i\mathrm{Tr}\,(\rho_{\mathrm{aux}}\,[\mathcal{H},\rho_0]) + \mathrm{Tr}\,(\rho_{\mathrm{aux}}\delta\mathcal{L}_1[\rho_0]) \tag{A1}$$

with

$$\mathcal{H} = \mathcal{H}_0 + \mathcal{H}_{int} = \sum_{\alpha\beta} t_{\alpha\beta} c^\dagger_\alpha c_\beta + \frac{1}{2}\sum_{\alpha\beta\gamma\delta} U_{\alpha\beta\gamma\delta} c^\dagger_\alpha c^\dagger_\beta c_\gamma c_\delta \tag{A2}$$

and

$$\delta\mathcal{L}_1[\rho_0] = \sum_{abcd}\Gamma_{abcd}\left[c_c c_d \rho_0 c^\dagger_a c^\dagger_b - \frac{1}{2}\left\{c^\dagger_a c^\dagger_b c_c c_d, \rho_0\right\}\right] \tag{A3}$$

where we defined $\Gamma_{abcd} \equiv \sqrt{\kappa_{ba}\kappa_{cd}}$. Due to the gaussian nature of the state ρ_0, the goal is to bring the trace Eq. (A1) in the form

$$\mathrm{Tr}\,(\rho_{\mathrm{aux}}\mathcal{L}_1[\rho_0]) = \mathrm{Tr}\,(\rho_{\mathrm{aux}}\mathcal{L}_{HF}[\rho_0]) \tag{A4}$$

where $\mathcal{L}_{HF}$ is an effective Hartree-Fock Liouvillian containing only single particle terms. We see that the unitary term involving the non-interacting Hamiltonian $\mathcal{H}_0$ is already in this form so that we have to compute only the terms involving the interacting part of the Hamiltonian $\mathcal{H}_{int}$ and the many-body dissipator. Let us start from the interacting part of the Hamiltonian

$$\mathrm{Tr}\,(\rho_{\mathrm{aux}}\,[\mathcal{H}_{int},\rho_0]) = \sum_{abcd} U_{abcd}\mathrm{Tr}\,\left(\rho_{\mathrm{aux}}\left[c^\dagger_a c^\dagger_b c_c c_d, \rho_0\right]\right) \tag{A5}$$

We now express the right-hand side of Eq. (A5) as a trace over the gaussian state ρ_0

$$\mathrm{Tr}\,(\rho_{\mathrm{aux}}\,[\mathcal{H}_{int},\rho_0]) = \sum_{abcd} U_{abcd}\mathrm{Tr}\,\left(\rho_0\rho_{\mathrm{aux}} c^\dagger_a c^\dagger_b c_c c_d\right) - U_{abcd}\mathrm{Tr}\,\left(\rho_0 c^\dagger_a c^\dagger_b c_c c_d \rho_{\mathrm{aux}}\right). \tag{A6}$$

We now can compute the trace by taking all the contractions involving two fermionic lines. For the sake of this example we will assume, for simplicity, that the anomalous contractions are zero, namely $\mathrm{Tr}\left(\rho_0 c_a^\dagger c_b^\dagger\right) = \mathrm{Tr}\left(\rho_0 c_a c_b\right) = 0$. For example, the first term in the RHS of the previous equation reads

$$\mathrm{Tr}\left(\rho_0\rho_{\mathrm{aux}} c_a^\dagger c_b^\dagger c_c c_d\right) = \mathrm{Tr}\left(\rho_0\rho_{\mathrm{aux}} c_a^\dagger c_b^\dagger c_c c_d\right) + \mathrm{Tr}\left(\rho_0\rho_{\mathrm{aux}} c_a^\dagger c_b^\dagger c_c c_d\right) - \mathrm{Tr}\left(\rho_0\rho_{\mathrm{aux}} c_a^\dagger c_b^\dagger c_c c_d\right) - \mathrm{Tr}\left(\rho_0\rho_{\mathrm{aux}} c_a^\dagger c_b^\dagger c_c c_d\right) \tag{A7}$$

where, in each term, the sign in each term takes into account the parity of the permutation.
Each permutation can be written as

$$\mathrm{Tr}\left(\rho_0\rho_{\mathrm{aux}} c_a^\dagger c_b^\dagger c_c c_d\right) = \mathrm{Tr}\left(\rho_0 c_a^\dagger c_d\right) \sum_{\mathrm{contractions}} \mathrm{Tr}\left(\rho_0\rho_{\mathrm{aux}} c_b^\dagger c_c\right) \tag{A8}$$

where the summation over contractions on the RHS indicates the sum over all the possible contractions involving the extraction of two fermionic lines from the operator $\rho_{\mathrm{aux}} c_b^\dagger c_c$. It is straightforward to see that this summation exactly reconstructs the trace of the operator over ρ_0, namely

$$\mathrm{Tr}\left(\rho_0\rho_{\mathrm{aux}} c_a^\dagger c_b^\dagger c_c c_d\right) = \mathrm{Tr}\left(\rho_0 c_a^\dagger c_d\right) \mathrm{Tr}\left(\rho_0\rho_{\mathrm{aux}} c_b^\dagger c_c\right). \tag{A9}$$

By iterating the above procedure for all the terms, the first term in Eq. (A1) reads

$$\mathrm{Tr}\left(\rho_{\mathrm{aux}}\left[\mathcal{H},\rho_0\right]\right) = \mathrm{Tr}\left(\rho_{\mathrm{aux}}\left[\mathcal{H}_{HF}[\rho_0],\rho_0\right]\right) \tag{A10}$$

with

$$\mathcal{H}_{HF} = \sum_{ab} t_{ab} c_a^\dagger c_b + \frac{1}{2}\sum_{abcd}(U_{abcd} - U_{abdc})\left[\mathrm{Tr}\left(\rho_0 c_a^\dagger c_d\right) c_b^\dagger c_c + \mathrm{Tr}\left(\rho_0 c_b^\dagger c_c\right) c_a^\dagger c_d\right]. \tag{A11}$$

By using the properties of the interaction matrix elements $U_{abcd} = U_{badc}$ we get

$$\mathcal{H}_{HF} = \sum_{ab} t_{ab} c_a^\dagger c_b + \sum_{abcd}(U_{abcd} - U_{abdc})\mathrm{Tr}\left(\rho_0 c_a^\dagger c_d\right) c_b^\dagger c_c. \tag{A12}$$

By using the same contraction scheme to dissipator term in Eq. (A1), we obtain

$$\mathrm{Tr}\left(\rho_{\mathrm{aux}}\delta\mathcal{L}_1[\rho_0]\right) = \mathrm{Tr}\left(\rho_{\mathrm{aux}}\delta\mathcal{L}_{HF}[\rho_0]\right) \tag{A13}$$

with

$$\delta\mathcal{L}_{HF}[\rho_0] = \sum_{abcd}\left(\Gamma_{abcd} - \Gamma_{abdc}\right)\left(\mathrm{Tr}\left(\rho_0 c_a^\dagger c_d\right)\left[c_c\rho_0 c_b^\dagger - \frac{1}{2}\left\{c_b^\dagger c_c, \rho_0\right\}\right] + \left[(a\leftrightarrow b)\quad(c\leftrightarrow d)\right]\right) \tag{A14}$$

where the second term is obtained from the first one upon exchanging $(a\leftrightarrow b)$ and $(c\leftrightarrow d)$. The dissipator couplings Γ_{abcd} satisfy the same index permutation property of the interaction terms $\Gamma_{abcd} = \Gamma_{badc}$, so that

$$\delta\mathcal{L}_{HF}[\rho_0] = 2\sum_{abcd}\overline{\Gamma}_{abcd}\mathrm{Tr}\left(\rho_0 c_a^\dagger c_d\right)\left[c_c\rho_0 c_b^\dagger - \frac{1}{2}\left\{c_b^\dagger c_c, \rho_0\right\}\right], \tag{A15}$$

where we defined $\overline{\Gamma}_{abcd} \equiv \Gamma_{abcd} - \Gamma_{abdc}$. Eventually, the action reads

$$\mathcal{S} = \int dt\mathrm{Tr}\left[\rho_{\mathrm{aux}}\left(\partial_t\rho_0 - \mathcal{L}_1[\rho_0]\right)\right] = \int dt\mathrm{Tr}\left[\rho_{\mathrm{aux}}\left(\partial_t - \rho_0\mathcal{L}_{HF}[\rho_0]\right)\right] \tag{A16}$$

and by taking the variation with respect to ρ_{aux} we obtain that the variational density matrix evolves with the effective single particle Liouvillian

$$i\partial_t\rho_0(t) = -i\left[\mathcal{H}_{HF}[\rho_0],\rho_0(t)\right] + \delta\mathcal{L}_{HF}[\rho_0(t)]. \tag{A17}$$

Following the same procedure for normalized states, the $\alpha < 1$ case is straightforwardly obtained, leading to

$$\partial_t\rho_{0,\alpha}(t) = -i\left[\mathcal{H}_{HF}[\rho_{0,\alpha}],\rho_{0,\alpha}\right] + \alpha\delta\mathcal{L}_{HF}[\rho_{0,\alpha}] + (\alpha-1)\sum_{abcd}\overline{\Gamma}_{abcd}\mathrm{Tr}\left(\rho_{0,\alpha}(t)c_a^\dagger c_d\right)\left\{c_b^\dagger c_c, \rho_{0,\alpha}\right\}. \tag{A18}$$

Appendix B: Hybrid DMVP for superconductivity with many-body dissipation

In this section, we discuss the detailed derivation of the hybrid BCS Liouvillian introduced in Sec. IV A of the main text. We consider only the case of two-body pumps as the loss-case is derived by particle-hole transformation. In order to apply the hybrid DMVP we compute the action by calculating the trace of the Liouvillian over the auxiliary state ρ_{aux}

$$\frac{\mathrm{Tr}\,(\rho_{\mathrm{aux}}\mathcal{L}_\alpha[\rho_{0,\alpha}])}{\mathrm{Tr}\,(\rho_{0,\alpha})} = \mathrm{Tr}\,\left(\rho_{\mathrm{aux}}\mathcal{L}_\alpha[\overline{\rho}_{0,\alpha}]\right) = -i\mathrm{Tr}\,\left(\rho_{\mathrm{aux}}\left[\mathcal{H},\overline{\rho}_{0,\alpha}\right]\right) + \mathrm{Tr}\,\left(\rho_{\mathrm{aux}}\delta\mathcal{L}_\alpha[\overline{\rho}_{0,\alpha}]\right), \tag{B1}$$

with hybrid dissipator $\delta\mathcal{L}_\alpha$ defined by the jump operators $L_i = \sqrt{2P}c^\dagger_{i\uparrow}c^\dagger_{i\downarrow}$. In Eq. (B1) we defined the normalized variational density matrix as

$$\overline{\rho}_{0,\alpha} \equiv \frac{\rho_{0,\alpha}}{\mathrm{Tr}\,(\rho_{0,\alpha})}. \tag{B2}$$

As seen in the previous section, the first trace leads to the Hartree-Fock decoupling of the unitary Hamiltonian which, by inclusion of the anomalous contraction terms, is represented by the standard BCS unitary Liouvillian

$$\mathrm{Tr}\,\left(\rho_{\mathrm{aux}}\left[\mathcal{H},\overline{\rho}_{0,\alpha}\right]\right) = \mathrm{Tr}\,\left(\rho_{\mathrm{aux}}\left[H_{BCS,0},\overline{\rho}_{0,\alpha}\right]\right) \tag{B3}$$

where, upon defining the superconducting order parameter $\Delta(t) \equiv \mathrm{Tr}\,\left(\overline{\rho}_{0,\alpha}c^\dagger_{i\uparrow}c^\dagger_{i\downarrow}\right)$,

$$H_{BCS,0} = \sum_{ij\sigma} t_{ij}c^\dagger_{i\alpha}c_{j\sigma} - |U|\Delta(t)\sum_i c_{i\downarrow}c_{i\uparrow} + \mathrm{h.c.}. \tag{B4}$$

We now focus on the trace of the dissipator

$$\mathrm{Tr}\,\left(\rho_{\mathrm{aux}}\delta\mathcal{L}_\alpha[\overline{\rho}_{0,\alpha}]\right) = P\sum_i 2\alpha\mathrm{Tr}\,\left(\rho_{\mathrm{aux}}c^\dagger_{i\uparrow}c^\dagger_{i\downarrow}\overline{\rho}_{0,\alpha}c_{i\downarrow}c_{i\uparrow}\right) - \mathrm{Tr}\,\left(\rho_{\mathrm{aux}}c_{i\downarrow}c_{i\uparrow}c^\dagger_{i\uparrow}c^\dagger_{i\downarrow}\overline{\rho}_{0,\alpha}\right) - \mathrm{Tr}\,\left(\rho_{\mathrm{aux}}\overline{\rho}_{0,\alpha}c_{i\downarrow}c_{i\uparrow}c^\dagger_{i\uparrow}c^\dagger_{i\downarrow}\right) \tag{B5}$$

We decoupled the trace in Eq. (B5) in both normal and anomalous channels. The three contributions become

$$\begin{aligned}\mathrm{Tr}\,\left(\rho_{\mathrm{aux}}c^\dagger_{i\uparrow}c^\dagger_{i\downarrow}\overline{\rho}_{0,\alpha}c_{i\downarrow}c_{i\uparrow}\right) &= \mathrm{Tr}\,\left(\overline{\rho}_{0,\alpha}c_{i\downarrow}c^\dagger_{i\downarrow}\right)\mathrm{Tr}\,\left(\overline{\rho}_{0,\alpha}c_{i\uparrow}\rho_{\mathrm{aux}}c^\dagger_{i\uparrow}\right) + \mathrm{Tr}\,\left(\overline{\rho}_{0,\alpha}c_{i\uparrow}c^\dagger_{i\uparrow}\right)\mathrm{Tr}\,\left(\overline{\rho}_{0,\alpha}c_{i\downarrow}\rho_{\mathrm{aux}}c^\dagger_{i\downarrow}\right)\\ &\quad + \mathrm{Tr}\,\left(\overline{\rho}_{0,\alpha}c_{i\downarrow}c_{i\uparrow}\right)\mathrm{Tr}\,\left(\overline{\rho}_{0,\alpha}\rho_{\mathrm{aux}}c^\dagger_{i\uparrow}c^\dagger_{i\downarrow}\right) + \mathrm{Tr}\,\left(\overline{\rho}_{0,\alpha}c^\dagger_{i\uparrow}c^\dagger_{i\downarrow}\right)\mathrm{Tr}\,\left(\overline{\rho}_{0,\alpha}c_{i\downarrow}c_{i\uparrow}\rho_{\mathrm{aux}}\right)\\ &= \left(1-\frac{n}{2}\right)\mathrm{Tr}\,\left(\rho_{\mathrm{aux}}c^\dagger_{i\uparrow}\overline{\rho}_{0,\alpha}c_{i\uparrow}\right) + \left(1-\frac{n}{2}\right)\mathrm{Tr}\,\left(\rho_{\mathrm{aux}}c^\dagger_{i\downarrow}\overline{\rho}_{0,\alpha}c_{i\downarrow}\right) + \Delta^*\mathrm{Tr}\,\left(\rho_{\mathrm{aux}}c^\dagger_{i\uparrow}c^\dagger_{i\downarrow}\overline{\rho}_{0,\alpha}\right) + \Delta\mathrm{Tr}\,\left(\rho_{\mathrm{aux}}\overline{\rho}_{0,\alpha}c_{i\downarrow}c_{i\uparrow}\right)\end{aligned} \tag{B6}$$

$$\begin{aligned}\mathrm{Tr}\,\left(\rho_{\mathrm{aux}}c_{i\downarrow}c_{i\uparrow}c^\dagger_{i\uparrow}c^\dagger_{i\downarrow}\overline{\rho}_{0,\alpha}\right) &= \mathrm{Tr}\,\left(\overline{\rho}_{0,\alpha}c_{i\downarrow}c^\dagger_{i\downarrow}\right)\mathrm{Tr}\,\left(\overline{\rho}_{0,\alpha}\rho_{\mathrm{aux}}c_{i\uparrow}c^\dagger_{i\uparrow}\right) + \mathrm{Tr}\,\left(\overline{\rho}_{0,\alpha}c_{i\uparrow}c^\dagger_{i\uparrow}\right)\mathrm{Tr}\,\left(\overline{\rho}_{0,\alpha}\rho_{\mathrm{aux}}c_{i\downarrow}c^\dagger_{i\downarrow}\right)\\ &\quad + \mathrm{Tr}\,\left(\overline{\rho}_{0,\alpha}c_{i\downarrow}c_{i\uparrow}\right)\mathrm{Tr}\,\left(\overline{\rho}_{0,\alpha}\rho_{\mathrm{aux}}c^\dagger_{i\uparrow}c^\dagger_{i\downarrow}\right) + \mathrm{Tr}\,\left(\overline{\rho}_{0,\alpha}c^\dagger_{i\uparrow}c^\dagger_{i\downarrow}\right)\mathrm{Tr}\,\left(\overline{\rho}_{0,\alpha}\rho_{\mathrm{aux}}c_{i\downarrow}c_{i\uparrow}\right)\\ &= \left(1-\frac{n}{2}\right)\mathrm{Tr}\,\left(\rho_{\mathrm{aux}}c_{i\uparrow}c^\dagger_{i\uparrow}\overline{\rho}_{0,\alpha}\right) + \left(1-\frac{n}{2}\right)\mathrm{Tr}\,\left(\rho_{\mathrm{aux}}c_{i\downarrow}c^\dagger_{i\downarrow}\overline{\rho}_{0,\alpha}\right) + \Delta^*\mathrm{Tr}\,\left(\rho_{\mathrm{aux}}c^\dagger_{i\uparrow}c^\dagger_{i\downarrow}\overline{\rho}_{0,\alpha}\right) + \Delta\mathrm{Tr}\,\left(\rho_{\mathrm{aux}}c_{i\downarrow}c_{i\uparrow}\overline{\rho}_{0,\alpha}\right)\end{aligned} \tag{B7}$$

$$\begin{aligned}\mathrm{Tr}\,\left(\rho_{\mathrm{aux}}\overline{\rho}_{0,\alpha}c_{i\downarrow}c_{i\uparrow}c^\dagger_{i\uparrow}c^\dagger_{i\downarrow}\right) &= \mathrm{Tr}\,\left(\overline{\rho}_{0,\alpha}c_{i\downarrow}c^\dagger_{i\downarrow}\right)\mathrm{Tr}\,\left(\overline{\rho}_{0,\alpha}c_{i\uparrow}c^\dagger_{i\uparrow}\rho_{\mathrm{aux}}\right) + \mathrm{Tr}\,\left(\overline{\rho}_{0,\alpha}c_{i\uparrow}c^\dagger_{i\uparrow}\right)\mathrm{Tr}\,\left(\overline{\rho}_{0,\alpha}c_{i\downarrow}c^\dagger_{i\downarrow}\rho_{\mathrm{aux}}\right)\\ &\quad + \mathrm{Tr}\,\left(\overline{\rho}_{0,\alpha}c_{i\downarrow}c_{i\uparrow}\right)\mathrm{Tr}\,\left(\overline{\rho}_{0,\alpha}c^\dagger_{i\uparrow}c^\dagger_{i\downarrow}\rho_{\mathrm{aux}}\right) + \mathrm{Tr}\,\left(\overline{\rho}_{0,\alpha}c^\dagger_{i\uparrow}c^\dagger_{i\downarrow}\right)\mathrm{Tr}\,\left(\overline{\rho}_{0,\alpha}c_{i\downarrow}c_{i\uparrow}\rho_{\mathrm{aux}}\right)\\ &= \left(1-\frac{n}{2}\right)\mathrm{Tr}\,\left(\rho_{\mathrm{aux}}\overline{\rho}_{0,\alpha}c^\dagger_{i\uparrow}c_{i\uparrow}\right) + \left(1-\frac{n}{2}\right)\mathrm{Tr}\,\left(\rho_{\mathrm{aux}}\overline{\rho}_{0,\alpha}c^\dagger_{i\downarrow}c_{i\downarrow}\right) + \Delta^*\mathrm{Tr}\,\left(\rho_{\mathrm{aux}}\overline{\rho}_{0,\alpha}c^\dagger_{i\uparrow}c^\dagger_{i\downarrow}\right) + \Delta\mathrm{Tr}\,\left(\rho_{\mathrm{aux}}\overline{\rho}_{0,\alpha}c_{i\downarrow}c_{i\uparrow}\right)\end{aligned} \tag{B8}$$

In the above equations $n \equiv \sum_\sigma \mathrm{Tr}\left(\overline{\rho}_{0,\alpha} c^\dagger_{i\sigma} c_{i\sigma}\right)$, and we assumed spin-unpolarized density $\mathrm{Tr}\left(\overline{\rho}_{0,\alpha} c^\dagger_{i\uparrow} c_{i\uparrow}\right) = \mathrm{Tr}\left(\overline{\rho}_{0,\alpha} c^\dagger_{i\downarrow} c_{i\downarrow}\right)$. By inserting Eqs. (B6)-(B8) into Eq. (B5), we obtain

$$\mathrm{Tr}\left(\rho_{\mathrm{aux}}\delta\mathcal{L}_\alpha[\overline{\rho}_{0,\alpha}]\right) = \left(1-\frac{n}{2}\right)\mathrm{Tr}\left(\rho_{\mathrm{aux}}\delta\mathcal{L}^{1-\mathrm{p}}_\alpha\right) + 2(\alpha-1)P\sum_i\left[\Delta\mathrm{Tr}\left(\rho_{\mathrm{aux}}\overline{\rho}_{0,\alpha}c_{i\downarrow}c_{i\uparrow}\right) + \Delta^*\mathrm{Tr}\left(\rho_{\mathrm{aux}}c^\dagger_{i\uparrow}c^\dagger_{i\downarrow}\overline{\rho}_{0,\alpha}\right)\right] - P\Delta\mathrm{Tr}\left(\rho_{\mathrm{aux}}\left[c_{i\downarrow}c_{i\uparrow},\overline{\rho}_{0,\alpha}\right]\right) + P\Delta^*\mathrm{Tr}\left(\rho_{\mathrm{aux}}\left[c^\dagger_{i\uparrow}c^\dagger_{i\downarrow},\overline{\rho}_{0,\alpha}\right]\right), \tag{B9}$$

where $\delta\mathcal{L}^{1-\mathrm{p}}_\alpha$ represents the hybrid single-particle pump dissipator

$$\delta\mathcal{L}^{1-\mathrm{p}}_\alpha = 2P\sum_{i\sigma}\left(\alpha c^\dagger_{i\sigma}\overline{\rho}_{0,\alpha}c_{i\sigma} - \frac{1}{2}\left\{c_{i\sigma}c^\dagger_{i\sigma},\overline{\rho}_{0,\alpha}\right\}\right). \tag{B10}$$

Putting all the terms together, the trace in Eq. (B1) becomes

$$\mathrm{Tr}\left(\rho_{\mathrm{aux}}\mathcal{L}_\alpha[\overline{\rho}_{0,\alpha}]\right) = \mathrm{Tr}\left(\rho_{\mathrm{aux}}\mathcal{L}^{\mathrm{pump}}_{BCS,\alpha}[\overline{\rho}_{0,\alpha}]\right) = -i\frac{\mathrm{Tr}\left(\rho_{\mathrm{aux}}H_{BCS}(P),\rho_{0,\alpha}\right)}{\mathrm{Tr}\left(\rho_{0,\alpha}\right)} + \frac{\mathrm{Tr}\left(\rho_{\mathrm{aux}}\delta\mathcal{L}^{\mathrm{pump}}_{BCS,\alpha}[\rho_{0,\alpha}]\right)}{\mathrm{Tr}\left(\rho_{0,\alpha}\right)} \tag{B11}$$

with BCS effective unitary Hamiltonian

$$H_{BCS}(P) = H_{BCS,0} - iP\Delta\sum_i c_{i\downarrow}c_{i\uparrow} + \mathrm{h.c.} \tag{B12}$$

and BCS effective dissipator

$$\delta\mathcal{L}^{\mathrm{pump}}_{BCS,\alpha} = \left(1-\frac{n}{2}\right)\delta\mathcal{L}^{1-\mathrm{p}}_\alpha + 2(\alpha-1)P\sum_i\left[\Delta\rho_{0,\alpha}c_{i\downarrow}c_{i\uparrow} + \Delta^*\mathrm{Tr}\,c^\dagger_{i\uparrow}c^\dagger_{i\downarrow}\rho_{0,\alpha}\right]. \tag{B13}$$

Inclusion of two-body loss leads to extra terms that can be obtained from Eq. (B9) upon particle-hole transformation. Eventually, variation of with respect to ρ_{aux} leads to the variational dynamics presented in the main text.

Appendix C: Derivation of the equations of motion

We detail the calculation of the equations of motions for the observables. As before, we show only calculation for the pump case and derive the loss contribution from particle-hole symmetry. For a given operator $\hat{O}$, the equations of motions for the normalized expectation values read

$$\langle\hat{O}\rangle_\alpha(t) = \mathrm{Tr}\left(\overline{\rho}_{0,\alpha}\hat{O}\right) = \frac{\mathrm{Tr}\left(\rho_{0,\alpha}\hat{O}\right)}{\mathrm{Tr}\left(\rho_{0,\alpha}\right)} \qquad \partial_t\langle\hat{O}\rangle_\alpha(t) = \mathrm{Tr}\left(\mathcal{L}^{\mathrm{pump}}_{BCS,\alpha}[\overline{\rho}_{0,\alpha}]\hat{O}\right) \tag{C1}$$

where, as explained in the Sec. IV B, the over the trace indicates that, in order to take into account the normalization, the calculation of the trace must include only contractions connecting fermionic operators belonging, respectively, to the Liouvillian and to the operator $\hat{O}$. To proceed, we rewrite the Liouvillian $\mathcal{L}^{\mathrm{pump}}_{BCS,\alpha}[\overline{\rho}_{0,\alpha}]$ as

$$\mathcal{L}^{\mathrm{pump}}_{BCS,\alpha}[\overline{\rho}_{0,\alpha}] = \mathcal{L}^{\mathrm{pump}}_{BCS,\alpha=1}[\overline{\rho}_{0,\alpha}] + 2P(\alpha-1)\left(1-\frac{n}{2}\right)\sum_{i\sigma}c^\dagger_{i\sigma}\overline{\rho}_{0,\alpha}c_{i\sigma} + 2P(\alpha-1)\sum_i\left[\Delta\rho_{0,\alpha}c_{i\downarrow}c_{i\uparrow} + \Delta^*\mathrm{Tr}\,c^\dagger_{i\uparrow}c^\dagger_{i\downarrow}\rho_{0,\alpha}\right], \tag{C2}$$

where $\mathcal{L}^{\mathrm{pump}}_{BCS,\alpha=1}$ is the BCS dissipator in the full Lindblad limit, and split the equations of motions in full Lindblad and hybrid, *i.e.* $\alpha \neq 1$, contributions

$$\partial_t\langle\hat{O}\rangle_\alpha = \left[\partial_t\langle\hat{O}\rangle_\alpha\right]_{\mathrm{Lindblad}} + (\alpha-1)\left[\partial_t\langle\hat{O}\rangle_\alpha\right]_{\mathrm{hybrid}} \tag{C3}$$

In the following, we consider $\hat{O} = c^\dagger_{\mathbf{k}\sigma}c_{\mathbf{k}\sigma}$ and $\hat{O} = c^\dagger_{\mathbf{k}\uparrow}c^\dagger_{-\mathbf{k}\downarrow}$. For simplicity, we remove the index α in the expectation values, namely $\Delta_{\mathbf{k}} \equiv \langle c^\dagger_{\mathbf{k}\uparrow}c^\dagger_{-\mathbf{k}\downarrow}\rangle_\alpha$ and $n_{\mathbf{k}\sigma} \equiv \langle c^\dagger_{\mathbf{k}\sigma}c_{-\mathbf{k}\sigma}\rangle_\alpha$. We also use the following symmetries $n_{\mathbf{k}\sigma} = n_{-\mathbf{k}\sigma}$, $n_{\mathbf{k}\uparrow} = n_{\mathbf{k}\downarrow}$ and $\Delta_{\mathbf{k}} = \Delta_{-\mathbf{k}}$. The Lindblad contributions are obtained by standard commutation relations

$$[\partial_t n_{\mathbf{k}\sigma}]_{\mathrm{Lindblad}} = -i\mathrm{Tr}\left(\overline{\rho}_{0,\alpha}\left[c^\dagger_{\mathbf{k}\sigma}c_{\mathbf{k}\sigma},H_{BCS}(P)\right]\right) + P\left(1-\frac{n}{2}\right)\sum_{i\sigma}\mathrm{Tr}\left(\overline{\rho}_{0,\alpha}c_{i\sigma}\left[c^\dagger_{\mathbf{k}\sigma}c_{\mathbf{k}\sigma},c^\dagger_{i\sigma}\right]\right) + \mathrm{Tr}\left(\overline{\rho}_{0,\alpha}\left[c_{i\sigma},c^\dagger_{\mathbf{k}\sigma}c_{\mathbf{k}\sigma}\right]c^\dagger_{i\sigma}\right) \tag{C4}$$

and

$$[\partial_t \Delta_{\mathbf{k}\sigma}]_{\text{Lindblad}} = -i\text{Tr}\left(\overline{\rho}_{0,\alpha}\left[c^\dagger_{\mathbf{k}\uparrow}c^\dagger_{-\mathbf{k}\downarrow}, H_{BCS}(P)\right]\right) + P\left(1-\frac{n}{2}\right)\sum_{i\sigma}\text{Tr}\left(\overline{\rho}_{0,\alpha}c_{i\sigma}\left[c^\dagger_{\mathbf{k}\uparrow}c^\dagger_{-\mathbf{k}\downarrow}, c^\dagger_{i\sigma}\right]\right) + \text{Tr}\left(\overline{\rho}_{0,\alpha}\left[c_{i\sigma}, c^\dagger_{\mathbf{k}\uparrow}c^\dagger_{-\mathbf{k}\downarrow}\right]c^\dagger_{i\sigma}\right), \tag{C5}$$

which, upon defining the complex gap amplitude $\Phi(P) = (-|U| + iP)\,\Delta$, become

$$[\partial_t n_{\mathbf{k}\sigma}]_{\text{Lindblad}} = -2\text{Im}\left[\Phi(P)\Delta_{\mathbf{k}}\right] + 2P\left(1-\frac{n}{2}\right)(1-n_{\mathbf{k}\sigma}) \tag{C6}$$

and

$$[\partial_t \Delta_{\mathbf{k}}]_{\text{Lindblad}} = i2\epsilon_{\mathbf{k}}\Delta_{\mathbf{k}} - i2\Phi(P)(2n_{\mathbf{k}\sigma}-1) - 2P\left(1-\frac{n}{2}\right)\Delta_{\mathbf{k}}. \tag{C7}$$

The hybrid contributions read

$$[\partial_t n_{\mathbf{k}\sigma}]_{\text{hybrid}} = 2P\left(1-\frac{n}{2}\right)\sum_{i\sigma'}\text{Tr}\left(\underbrace{c^\dagger_{i\sigma'}\overline{\rho}_{0,\alpha}c_{i\sigma'}}\underbrace{c^\dagger_{\mathbf{k}\sigma'}c_{\mathbf{k}\sigma'}}\right) + 2P\sum_i \Delta\text{Tr}\left(\underbrace{c^\dagger_{\mathbf{k}\sigma}c_{\mathbf{k}\sigma}}\underbrace{\rho_{0,\alpha}c_{i\downarrow}c_{i\uparrow}}\right) + \text{c.c.} \tag{C8}$$

$$\begin{aligned}[\partial_t \Delta_{\mathbf{k}}]_{\text{hybrid}} = 2P\left(1-\frac{n}{2}\right)\sum_{i\sigma}\text{Tr}\left(\underbrace{c^\dagger_{i\sigma}\overline{\rho}_{0,\alpha}c_{i\sigma}}\underbrace{c^\dagger_{\mathbf{k}\uparrow}c^\dagger_{-\mathbf{k}\downarrow}}\right) + 2P\sum_i \Delta\text{Tr}\left(\underbrace{c^\dagger_{\mathbf{k}\uparrow}c^\dagger_{-\mathbf{k}\downarrow}}\underbrace{\rho_{0,\alpha}c_{i\downarrow}c_{i\uparrow}}\right) + \\ \Delta^*\text{Tr}\left(\underbrace{c^\dagger_{\mathbf{k}\uparrow}c^\dagger_{-\mathbf{k}\downarrow}}\underbrace{c^\dagger_{i\uparrow}c^\dagger_{i\downarrow}\rho_{0,\alpha}}\right)\end{aligned} \tag{C9}$$

where the lines indicate contractions connecting fermionic operators on the two groups of operators. This can easily be computed with the help of translation and spin symmetry, $\langle c^\dagger_{\mathbf{k}\sigma}c_{\mathbf{k}'\sigma'}\rangle \propto \delta_{\mathbf{k}\mathbf{k}'}\delta_{\sigma\sigma'}$ and $\langle c^\dagger_{\mathbf{k}\sigma}c^\dagger_{\mathbf{k}'\sigma'}\rangle \propto \delta_{\mathbf{k}-\mathbf{k}'}\delta_{\sigma,-\sigma'}$, leading to

$$[\partial_t n_{\mathbf{k}\sigma}]_{\text{hybrid}} = 2P\left[\left(1-\frac{n}{2}\right)\left[(1-n_{\mathbf{k}\sigma})^2 - |\Delta_{\mathbf{k}}|^2\right] + 2\text{Re}[\Delta\Delta^*_{\mathbf{k}}](1-n_{\mathbf{k}\sigma})\right] \tag{C10}$$

and

$$[\partial_t \Delta_{\mathbf{k}}]_{\text{hybrid}} = 2P\left[(2-n)\,\Delta_{\mathbf{k}}(n_{\mathbf{k}\sigma}-1) + \Delta(1-n_{\mathbf{k}\sigma})^2 - \Delta^*\Delta^2_{\mathbf{k}}\right] \tag{C11}$$

The equations of motions for the losses are obtained by applying particle-hole transformations $\Delta_{\mathbf{k}} \to -\Delta^*_{\mathbf{k}}$, $n_{\mathbf{k}\sigma} \to (1-n_{\mathbf{k}\sigma})$ and leads to the full equations of motion presented in the main text.